Supporting Information

1. Materials and methods

All reagents and deuterated solvents were used as purchased without further purification. PDI-based ligand **1**[S1] was prepared according to the literature procedures. Ligand **2a** was synthesized by Suzuki coupling and hydrolysis reaction. Ligands **2b** and **2c** were purchased in the carboxylic acid form and obtained by neutralization reaction with NaOH.

2. Synthetic procedures and characterization data

*2.1 Synthesis of compound **9***

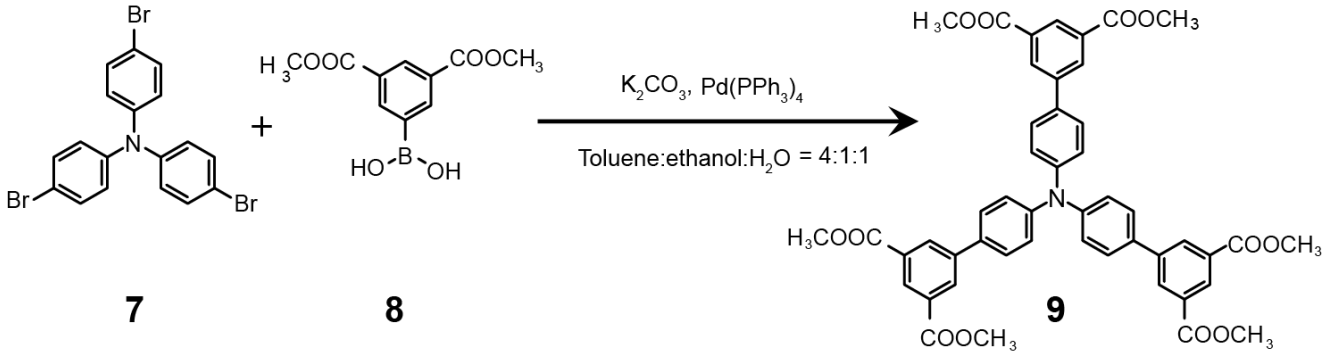

7 **8** **9**

Compound **7** (1.00 g, 2.07 mmol) was combined with (3,5-bis(ethoxycarbonyl)phenyl)boronic acid (2.96 mg, 12.45 mmol), anhydrous K_2CO_3 (399.4 mg, 24.90 mmol), and $Pd(PPh_3)_4$ (0.24 g, 0.2 mmol) in toluene (40.0 mL). To this mixture, H_2O (10 mL) and ethanol (10 mL) were added. The resulting reaction mixture was stirred at 85 °C for 48 hours under a nitrogen atmosphere. After cooling to room temperature, the product was concentrated to obtain a crude product. The crude product was purified by flash column chromatography using a CH_2Cl_2:Methanol (100:1) mixture as the eluent, yielding compound **9** (1.20 g, 70%) as a yellow solid. ^{1}H NMR (400 MHz, $CDCl_3$, 295 K) δ 8.63 (s, 3H), 8.46 (d, J = 1.3 Hz, 6H), 7.62 (d, J = 8.5 Hz, 6H), 7.28 (d, J = 8.5 Hz, 6H), 4.45 (q, J = 7.1 Hz, 18H).

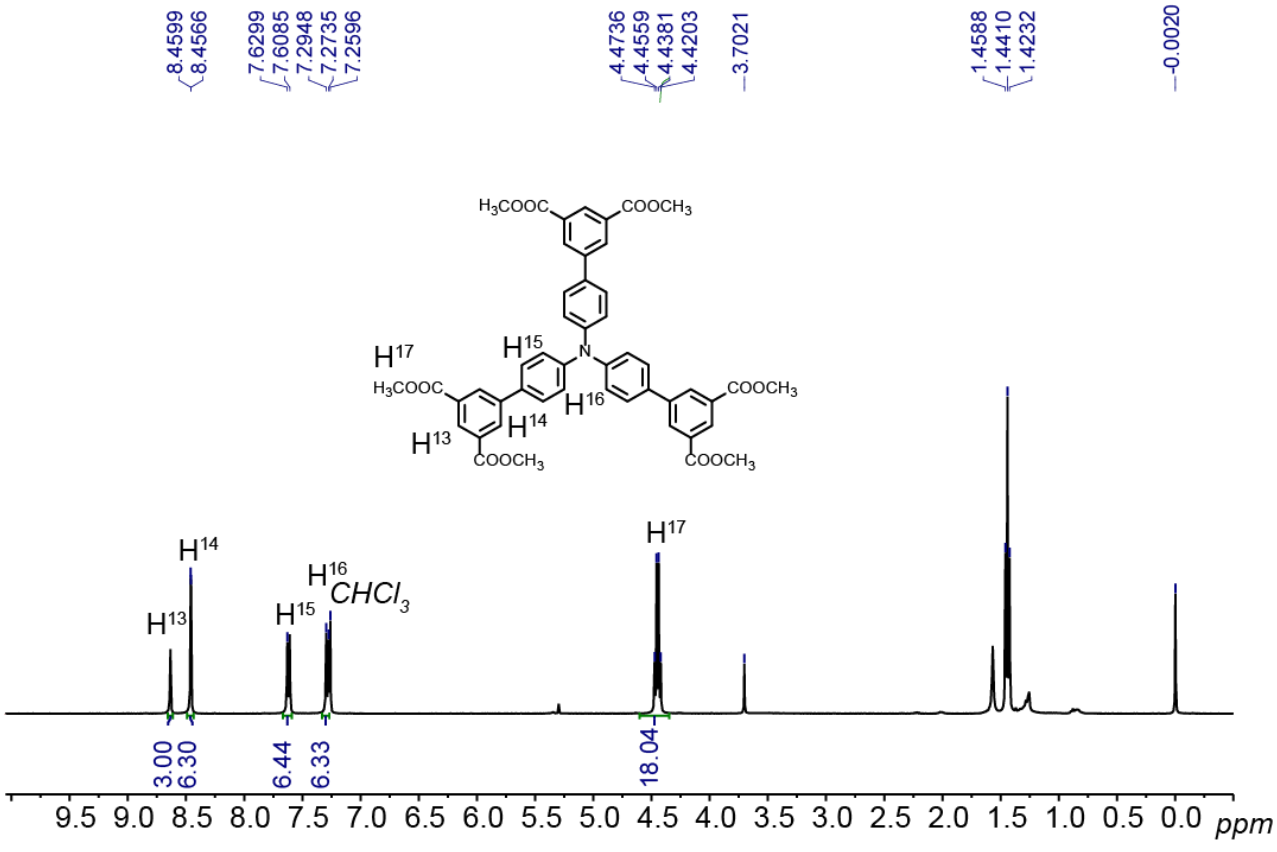

Figure S1. ^{1}H NMR spectrum (400 MHz, $CDCl_3$, 295 K) recorded for **9**.

*2.2 Synthesis of compound **10***

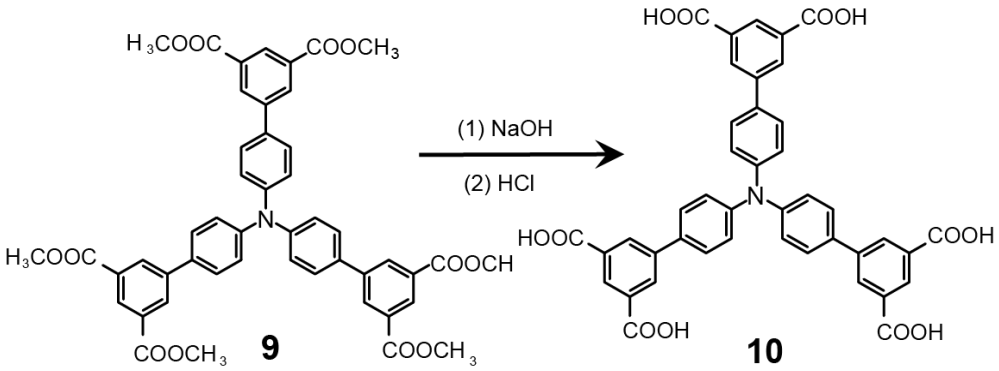

Compound **9** (1.00 g, 1.22 mmol) and NaOH (306.61 mg, 7.67 mmol) were added to a mixture of ethanol, THF, and water (24/24/6 mL). The resulting reaction mixture was stirred at 70 °C for 12 hours. After cooling to room temperature, the solvents were evaporated under reduced pressure, and the pH was adjusted to 4.0 using a 1.0 mM HCl solution. The yellow precipitate was filtered and washed with water (40 mL), yielding compound **10** (852.71 mg, 95%). ^{1}H NMR (400 MHz, DMSO-d*6*, 295 K) δ 13.47 (s, 6H), 8.67 (s, 3H), 8.41 (d, *J* = 1.4 Hz, 6H), 7.90 (dd, *J* = 7.0, 3.2 Hz, 6H), 7.54 (dd, *J* = 7.0, 3.1 Hz, 6H).

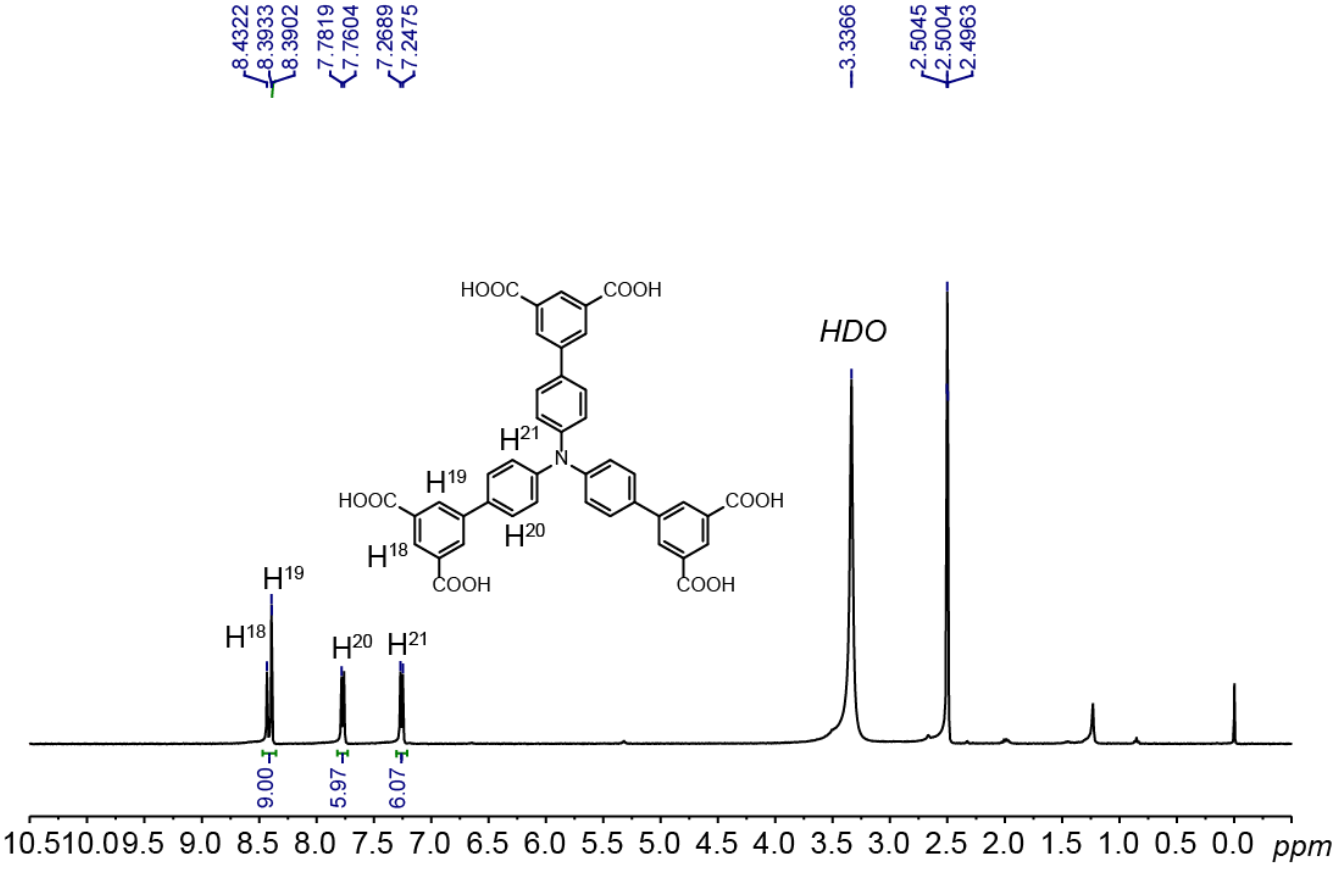

Figure S2. ^{1}H NMR spectrum (400 MHz, DMSO-d*6*, 295 K) recorded for **10**.

2.3 Synthesis of Ligand ***2a***

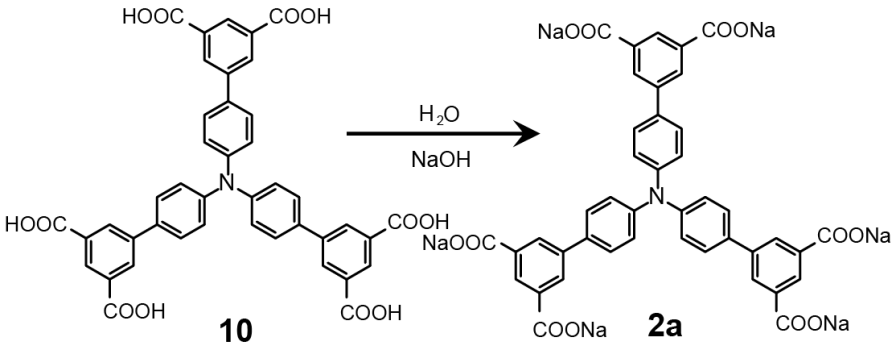

Compound **10** (300.00 mg, 0.47 mmol) and NaOH (117.65 mg, 2.94 mmol) were added to 30 mL of water and stirred at room temperature for 3 hours. The mixture was then concentrated and washed with acetone, resulting in the formation of **2a** (336.06 mg, 93%) as a white solid. ^{1}H NMR (400 MHz, CD_3OD, 295 K) δ 8.54 (s, 3H), 8.31 (d, J = 1.4 Hz, 6H), 7.70 (d, J = 8.6 Hz, 6H), 7.23 (d, J = 8.6 Hz, 6H).

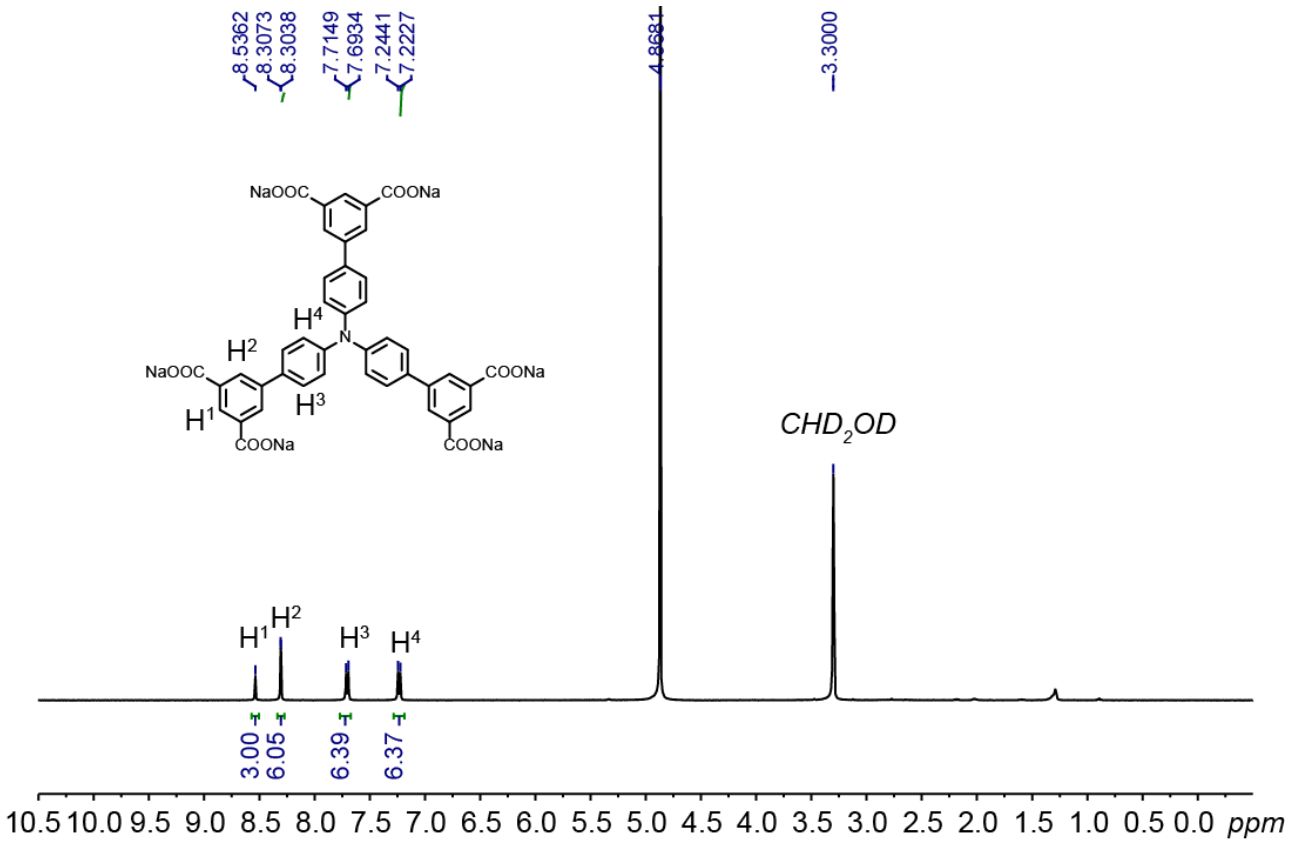

Figure S3. ^{1}H NMR spectrum (400 MHz, CD_3OD, 295 K) recorded for **2a**.

2.4 Synthesis of Ligand ***2b***

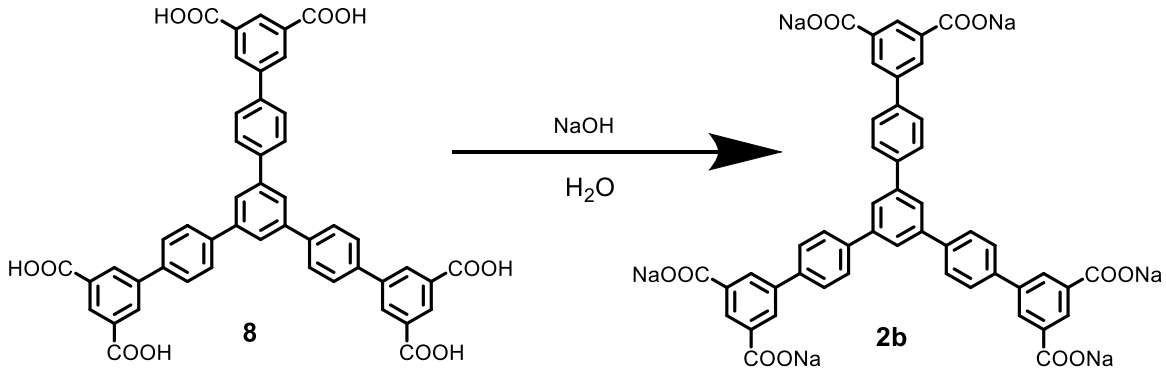

Compound **8** (300.00 mg, 0.38 mmol) and NaOH (94.64 mg, 2.37 mmol) were added to 30 mL of water and stirred at room temperature for 3 hours. The mixture was then concentrated and washed with acetone, resulting in the formation of **2b** (328.57 mg, 94%) as a white solid. ^{1}H NMR (400 MHz, CD_3OD, 295 K) δ 8.47 (s, 3H), 8.40 (d, *J* = 1.5 Hz, 6H), 7.99 (s, 3H), 7.94 (s, 12H).

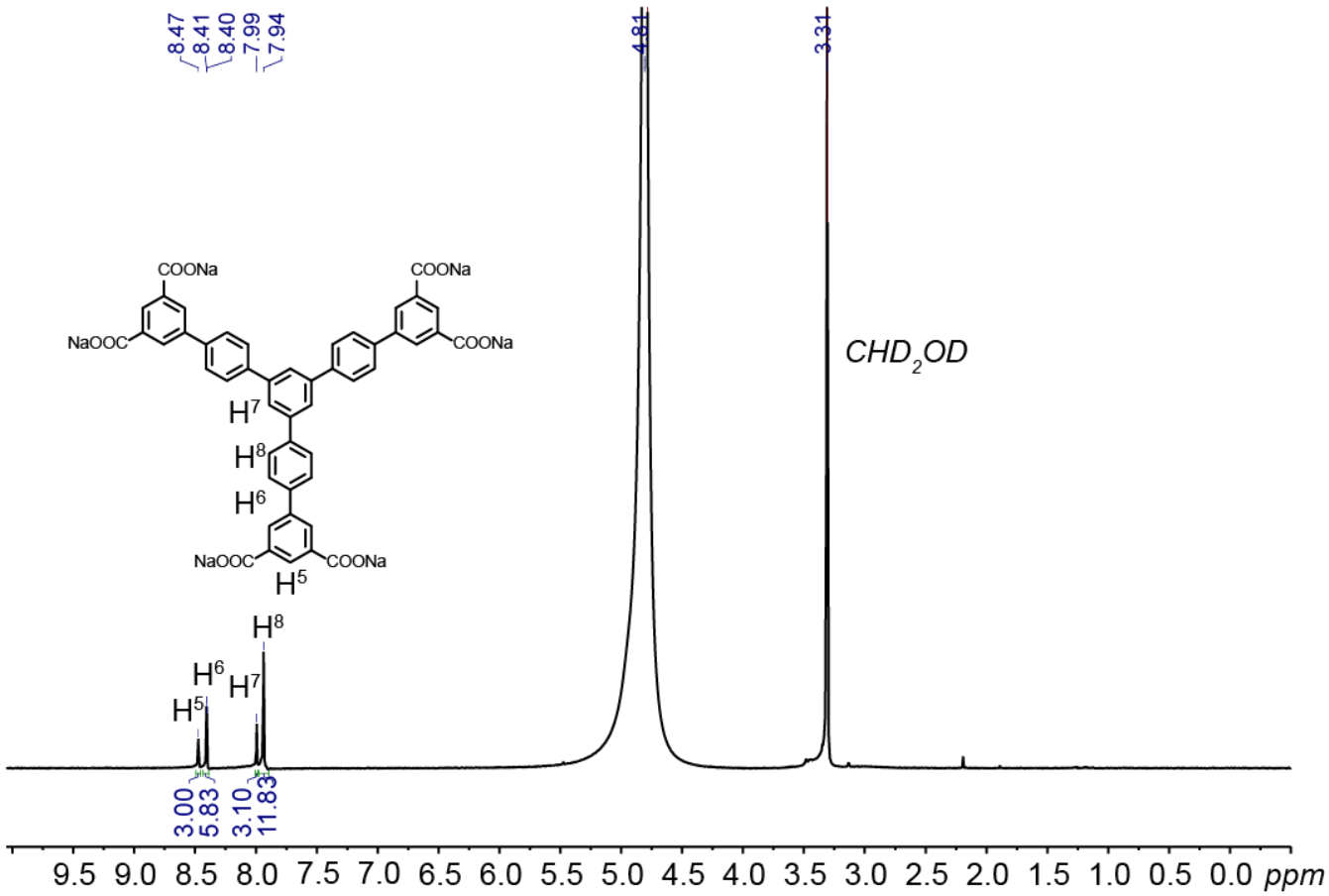

Figure S4. ^{1}H NMR spectrum (400 MHz, CD_3OD, 295 K) recorded for ligand **2b**.

2.5 Synthesis of Ligand ***2c***

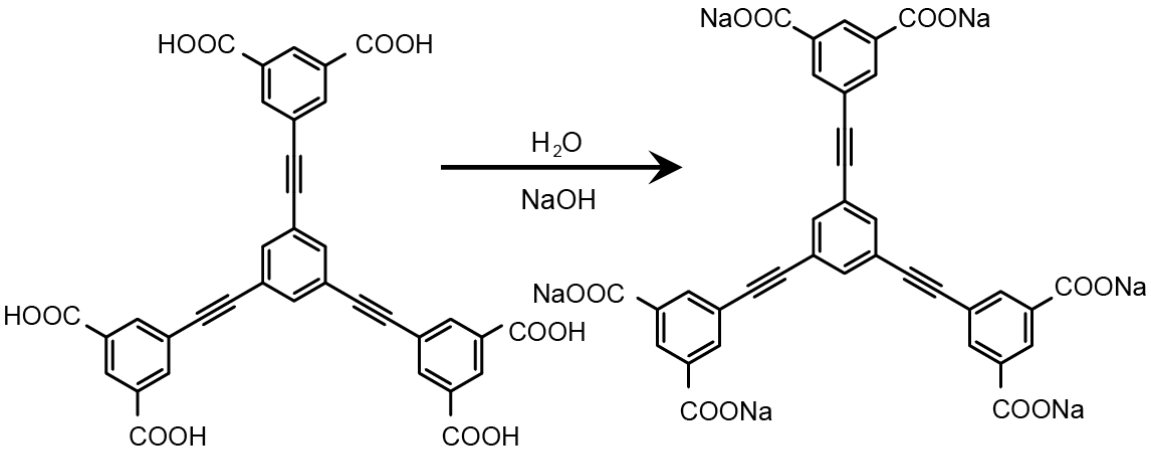

12 **2c**

Compound **12** (300.00 mg, 0.47 mmol) and NaOH (117.65 mg, 2.94 mmol) were added to 30 mL of water and stirred at room temperature for 3 hours. The mixture was then concentrated and washed with acetone, resulting in the formation of **2c** (336.06 mg, 93%) as a white solid. ^{1}H NMR (400 MHz, CD_3OD, 295 K) δ 8.39 (s, 3H), 8.15 (d, J = 1.4 Hz, 6H), 7.54 (s, 3H).

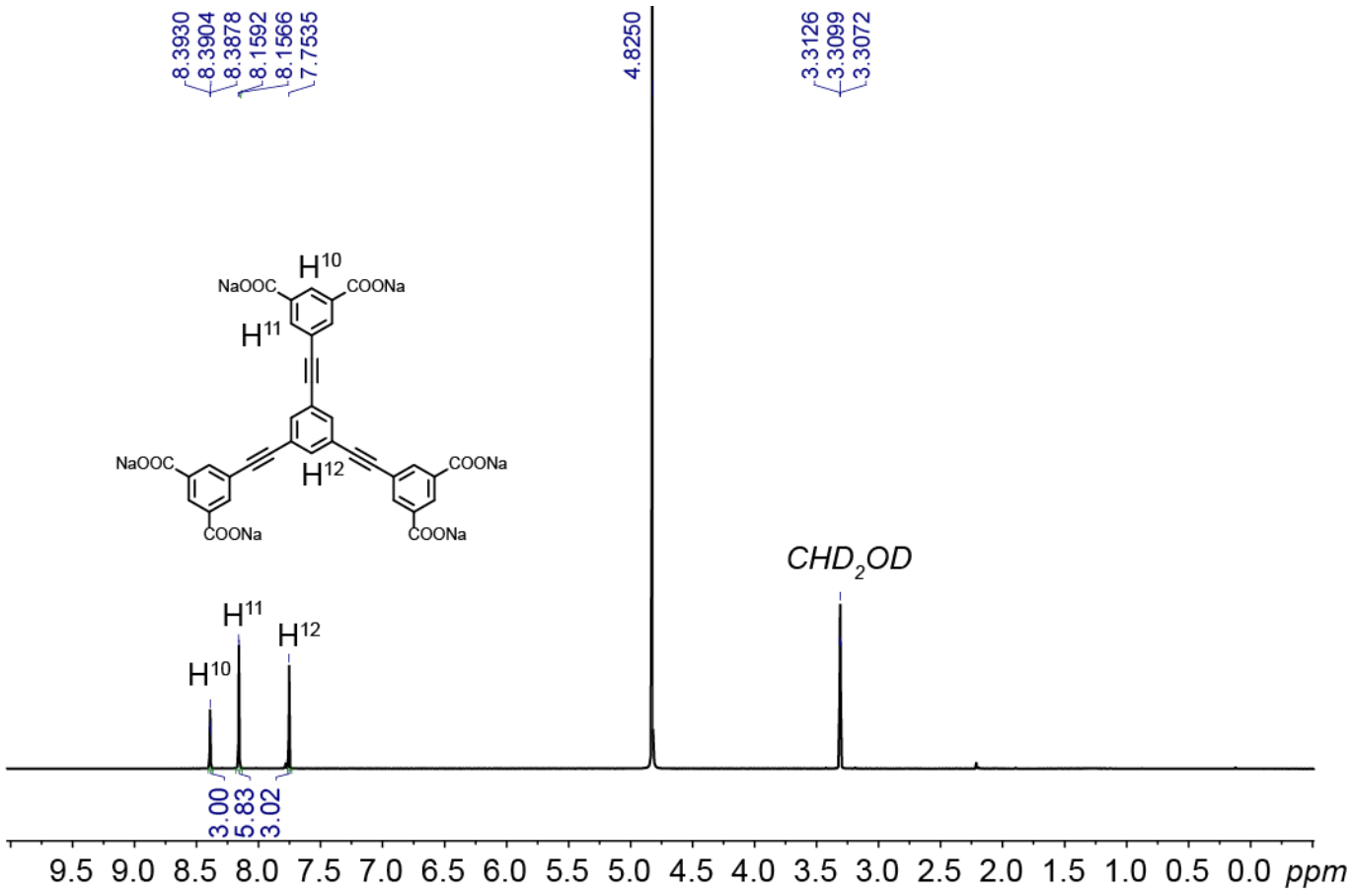

Figure S5. ^{1}H NMR spectrum (400 MHz, CD_3OD, 295 K) recorded for ligand **2c.**

*2.6 Self-assembly of metallacage **4a***

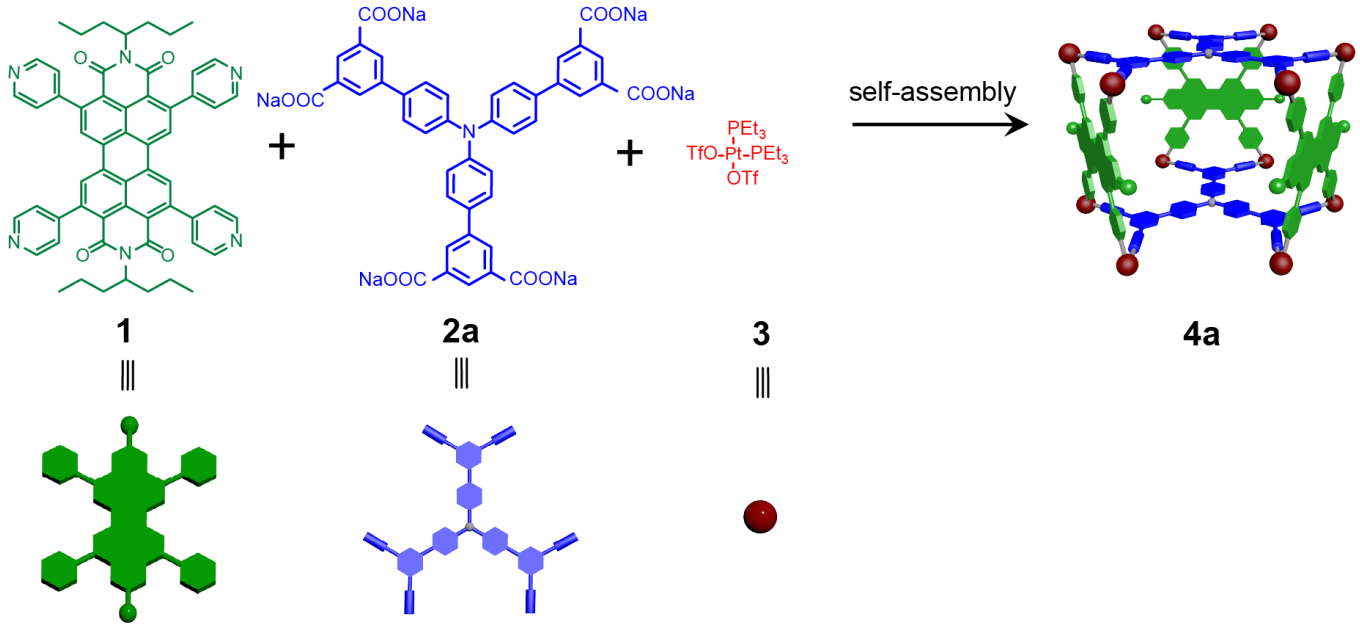

1 (3.00 mg, 3.35 μmol), **2a** (1.94 mg, 2.23 μmol) and **3** (9.78 mg, 13.41 μmol) were mixed in a 1:1:4 molar ratio and dissolved in acetone/water (20 mL, 4:1, *v*/*v*). The whole reaction mixture was heated at 50 ℃ for 12 hours and then cooled to room temperature. The solvent was removed by nitrogen flow. The residue was redissolved in CH_3CN (1.0 mL), filtered, and treated with ethyl ether (4 mL) to induce precipitation. The resulting precipitate was collected via centrifugation, yielding metallacage **4a** (47.05 mg, 95%) as a red solid. ^{1}H NMR (600 MHz, CD_3CN, 295 K) δ 9.00-9.02 (m, 12 H), 8.74–8.68 (m, 12 H), 8.39 (s, 12H), 8.21 (s, 6 H), 8.15 (d, J = 1.2 Hz, 12 H), 7.61 (d, J = 5.5 Hz, 12 H), 7.51 (d, J = 8.6 Hz, 12 H), 7.39 (d, J = 5.6 Hz, 12 H), 7.15 (d, J = 8.6 Hz, 12 H), 4.75 (ddd, J = 15.0, 9.2, 5.9 Hz, 12 H). ^{31}P{^{1}H} NMR (243 MHz, CD_3CN, 295 K): 5.15 ppm (d, $^2J_{P\text{-}P}$ =21.87 Hz, ^{195}Pt satellites, $^1J_{Pt\text{-}P}$ = 1612 Hz), –0.39 ppm (d, $^2J_{Pt\text{-}P}$ =21.87 Hz, ^{195}Pt satellites, $^1J_{Pt\text{-}P}$ = 1612 Hz). ESI-TOF-MS: *m/z* 1085.6512 [**4a** – 9OTf]$^{9+}$, 1240.0909 [**4a** – 8OTf]$^{8+}$, 1438.3900 [**4a** – 7OTf]$^{7+}$, 1702.7886 [**4a** – 6OTf]$^{6+}$and 2073.3660 [**4a** – 5OTf]$^{5+}$.

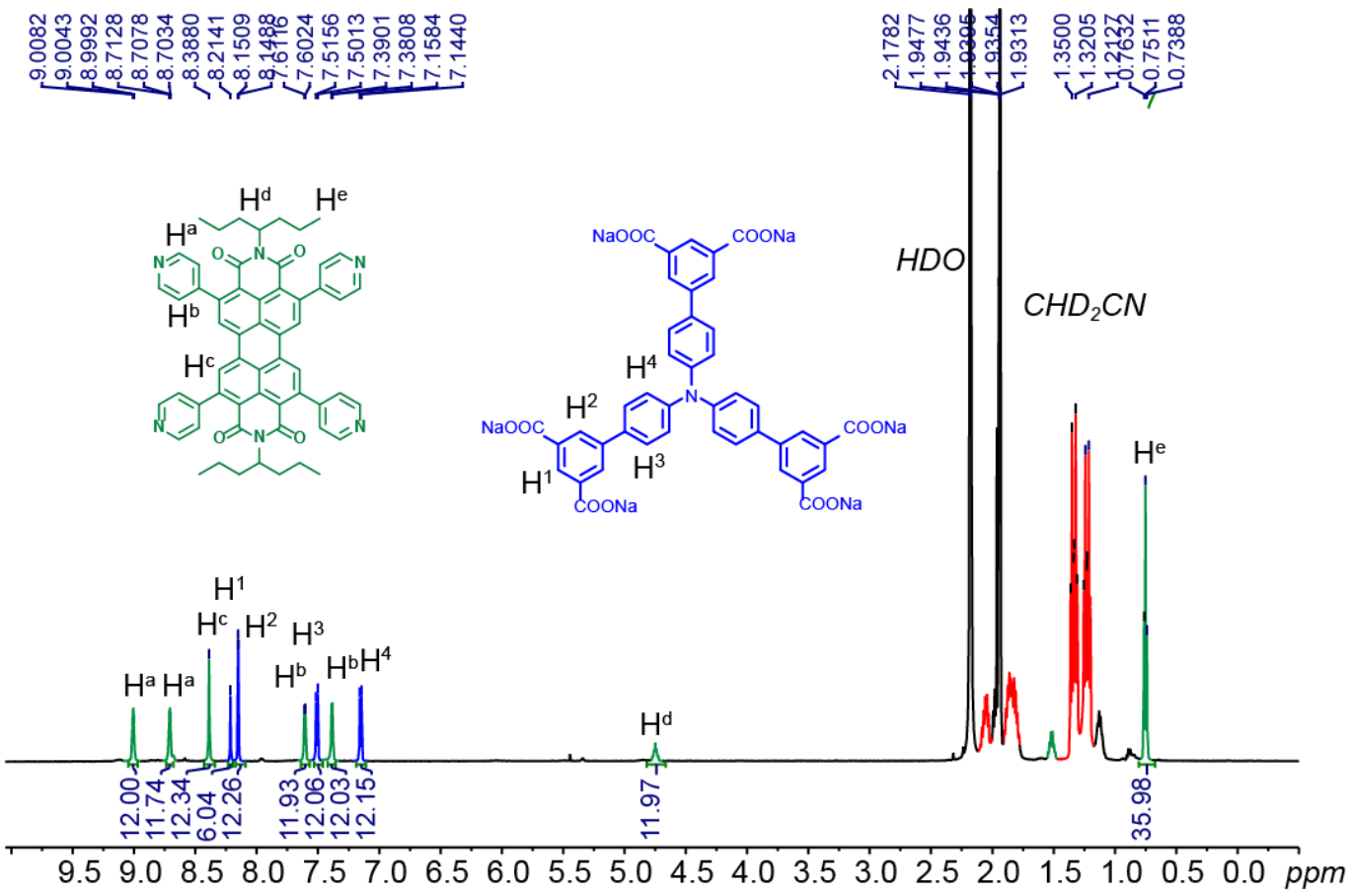

Figure S6. ^{1}H NMR spectrum (600 MHz, CD_3CN, 295 K) recorded for **4a**.

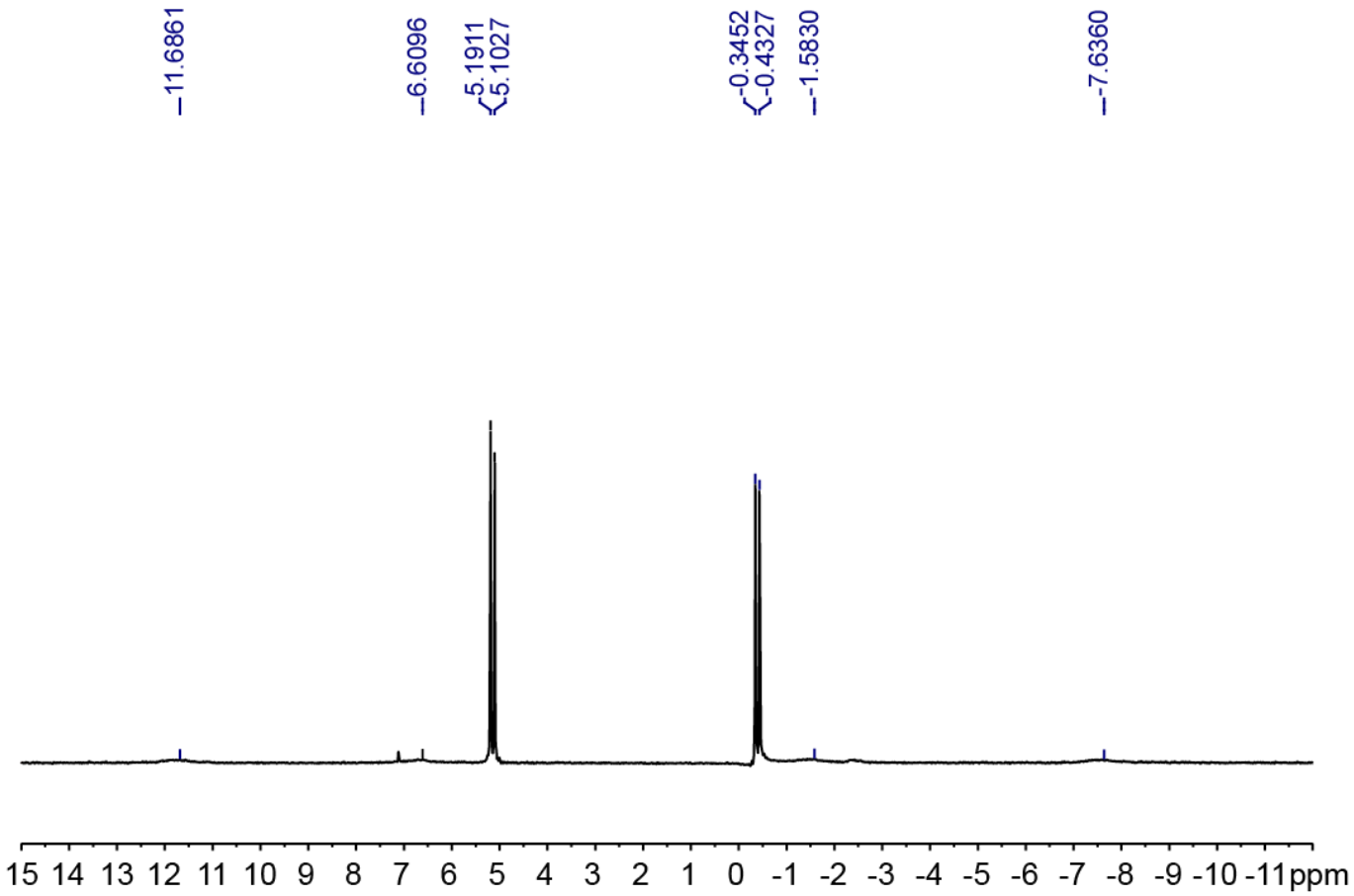

Figure S7. $^{31}P\{^{1}H\}$ NMR spectrum (162 MHz, CD_3CN, 295 K) recorded for **4a**.

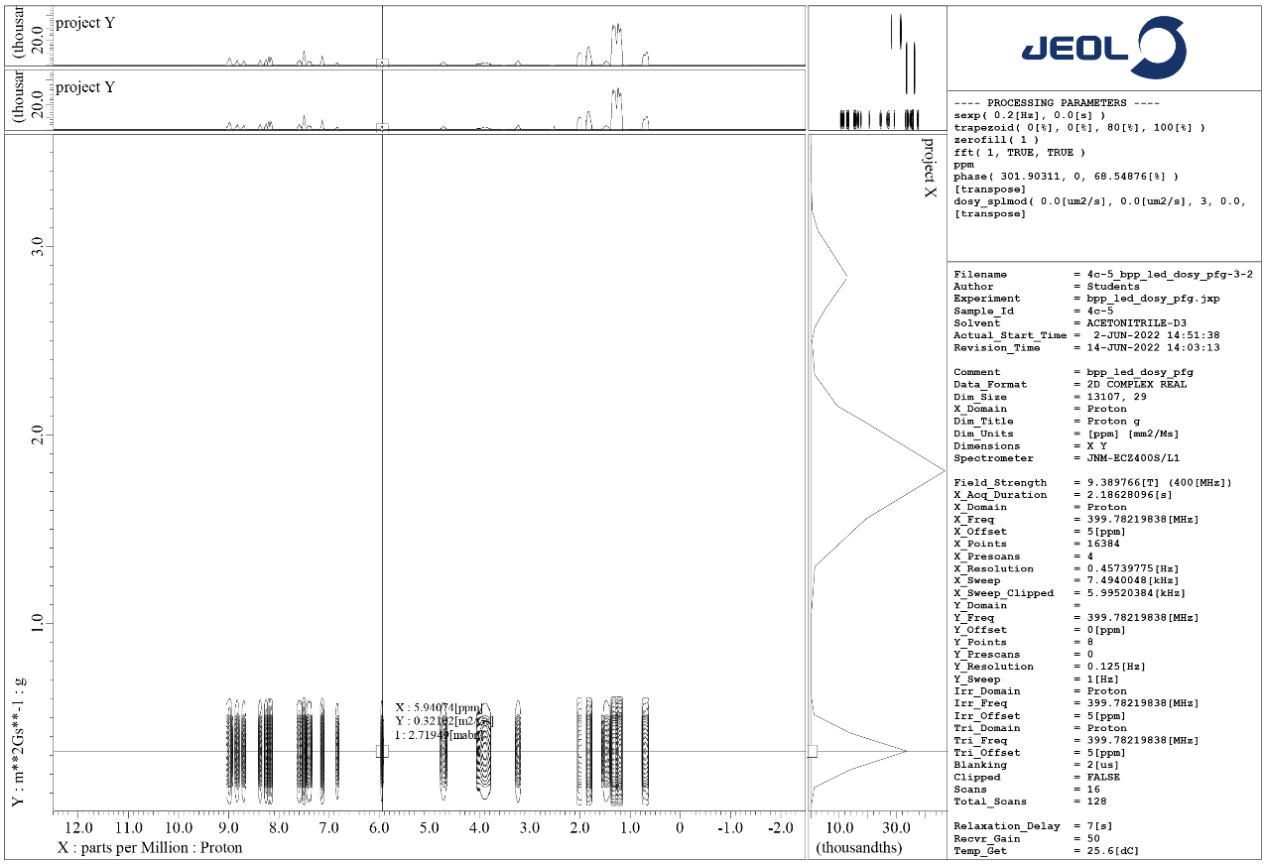

Figure S8. 2D ^{1}H DOSY spectra (400 MHz, CD_3CN, 295 K) recorded for metallacycle **4a.**

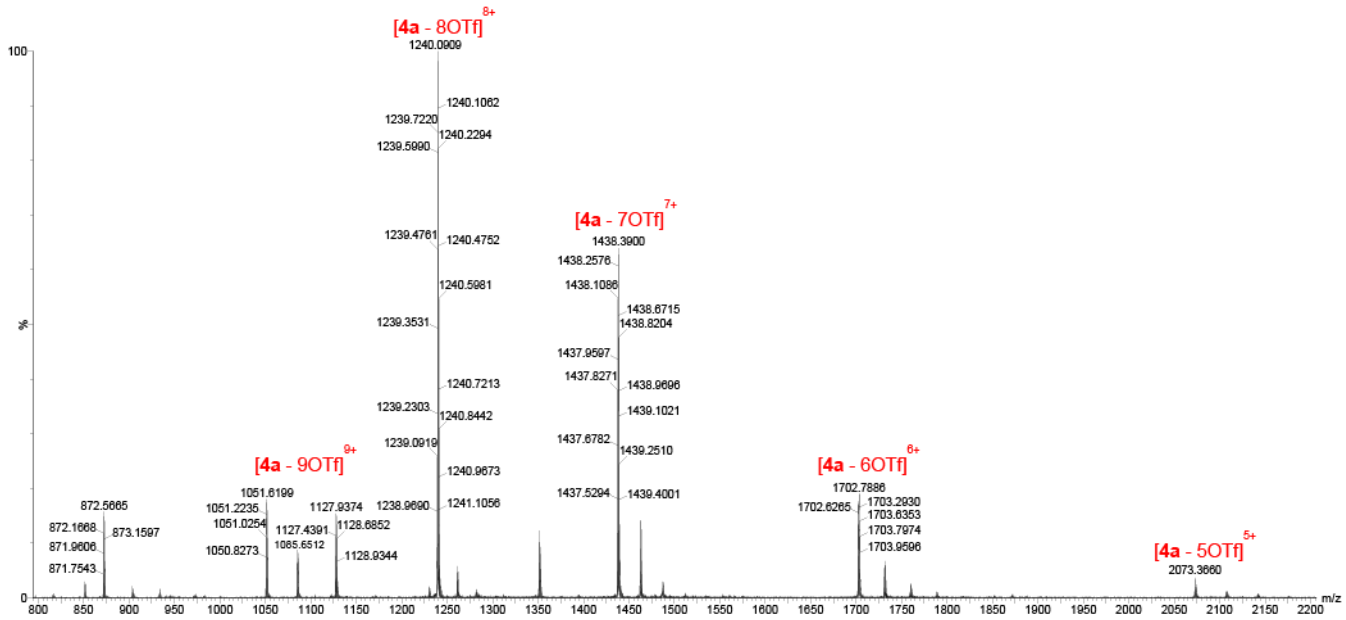

Figure S9. ESI-TOF-MS spectrum of **4a.**

*2.7 Self-assembly of metallacage **4b***

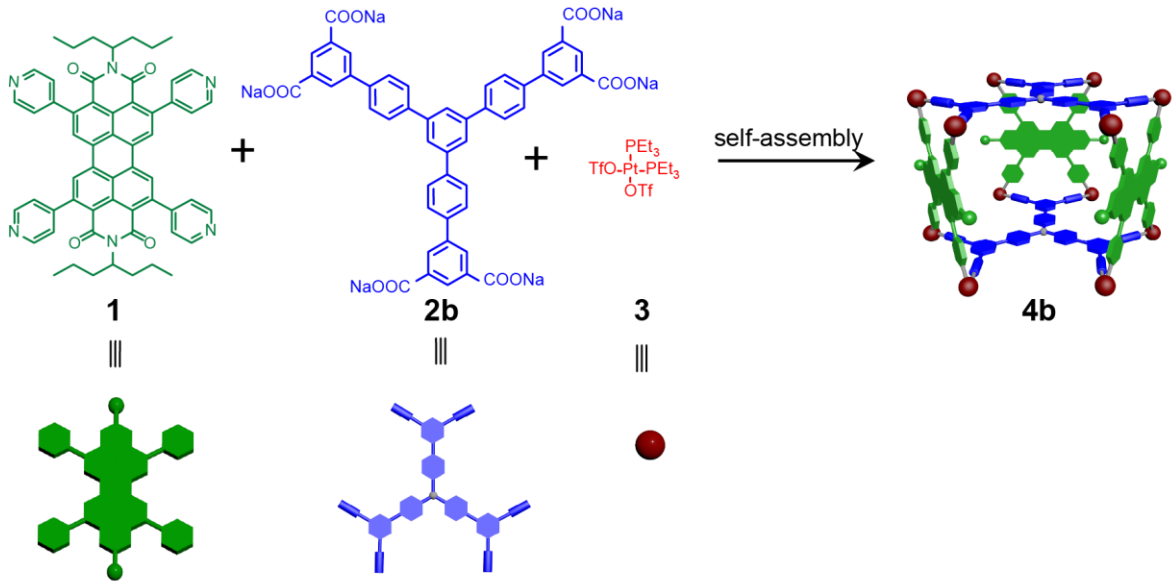

1 (10.00 mg, 11.17 μmol), **2b** (6.93 mg, 7.45 μmol) and **3** (32.60 mg, 44.69 μmol) were mixed in a 1:1:4 molar ratio and dissolved in acetone/water (20 mL, 4:1, *v*/*v*). The whole reaction mixture was heated at 50 ℃ for 12 hours and then cooled to room temperature. The solvent was removed by nitrogen flow. The residue was redissolved in CH_3CN (1.0 mL) and filtered, and then ethyl ether (4 mL) was added to give a precipitate, which was collected by centrifugation to give metallacage **4b** (47.05 mg, 95%) as a red solid. ^{1}H NMR (600 MHz, CD_3CN, 295 K) δ 9.05 (dd, J = 5.5, 3.0 Hz, 12H), 8.75 (d, J = 3.2 Hz, 12H), 8.46 (s, 12H), 8.33 (d, J = 1.3 Hz, 10H), 8.29 (s, 6H), 7.97 (s, 6H), 7.94 (d, J = 7.9 Hz, 11H), 7.79 (d, J = 8.1 Hz, 11H), 7.67 (d, J = 5.5 Hz, 12H), 7.41 (d, J = 5.8 Hz, 12H).^{31}P{^{1}H} NMR (243 MHz, CD_3CN, 295 K): 5.23 ppm (d, $^2J_{P\text{-}P}$ =21.58 Hz, ^{195}Pt satellites, $^1J_{Pt\text{-}P}$ = 1724 Hz), –0.31 ppm (d, $^2J_{P\text{-}P}$ =21.58 Hz, ^{195}Pt satellites, $^1J_{Pt\text{-}P}$ = 1724 Hz). ESI-TOF-MS: *m/z* 1099.3143 [**4b** – 9OTf]$^{9+}$, 1255.2319 [**4b** – 8OTf]$^{8+}$, 1455.8258 [**4b** – 7OTf]$^{7+}$, 1723.3123 [**4b** – 6OTf]$^{6+}$ and 2097.7883 [**4b** – 5OTf]$^{5+}$.

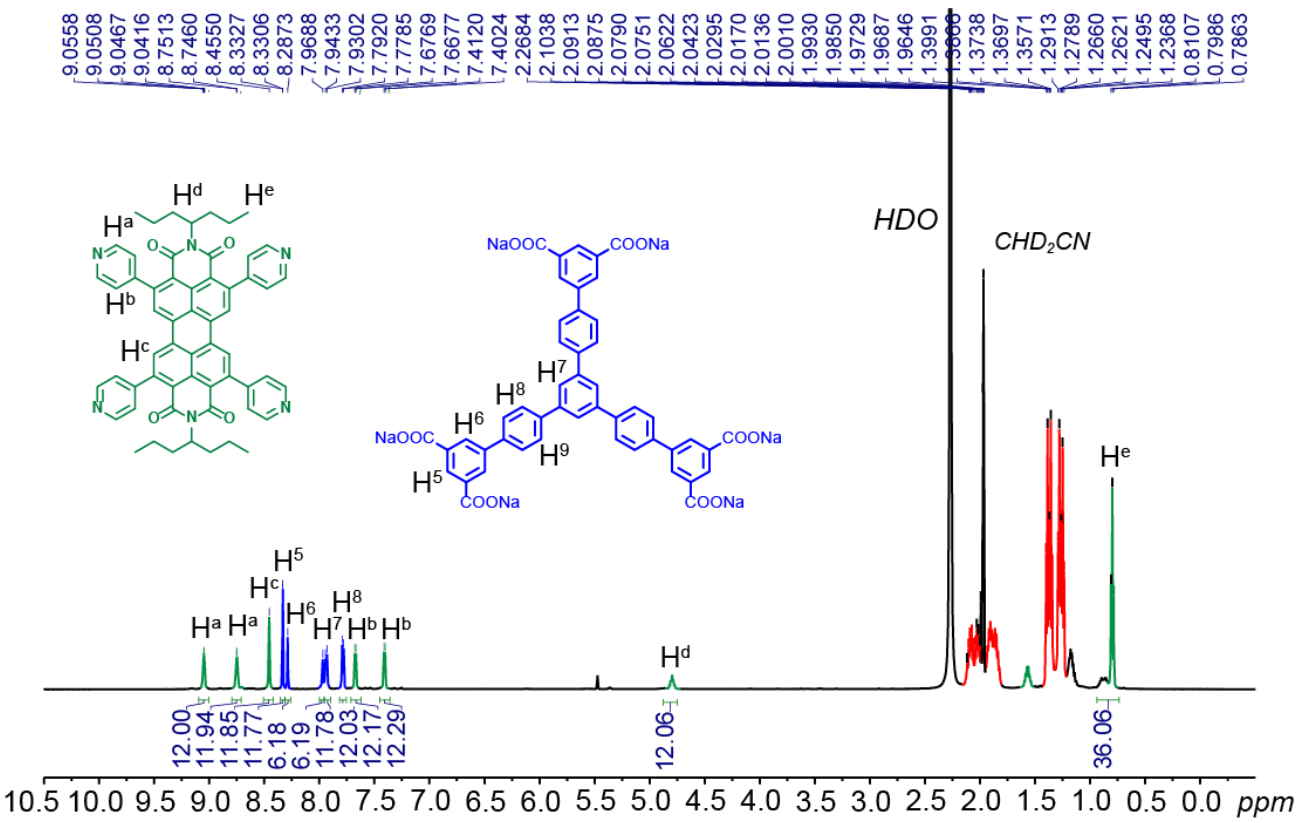

Figure S10. ^{1}H NMR spectrum (400 MHz, CD_3CN, 295 K) recorded for **4b**.

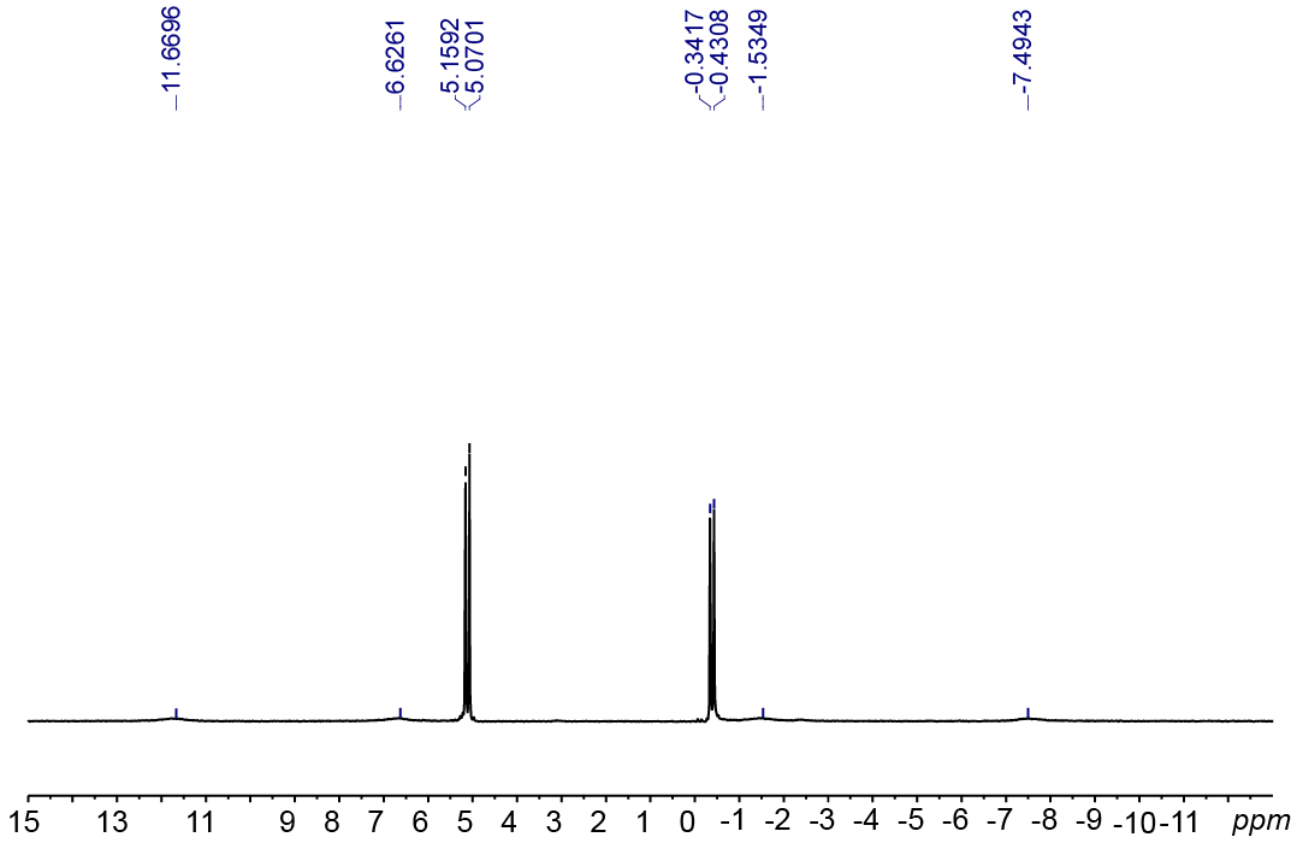

Figure S11. $^{31}P\{^{1}H\}$ NMR spectrum (162 MHz, CD_3CN, 295 K) recorded for **4b**.

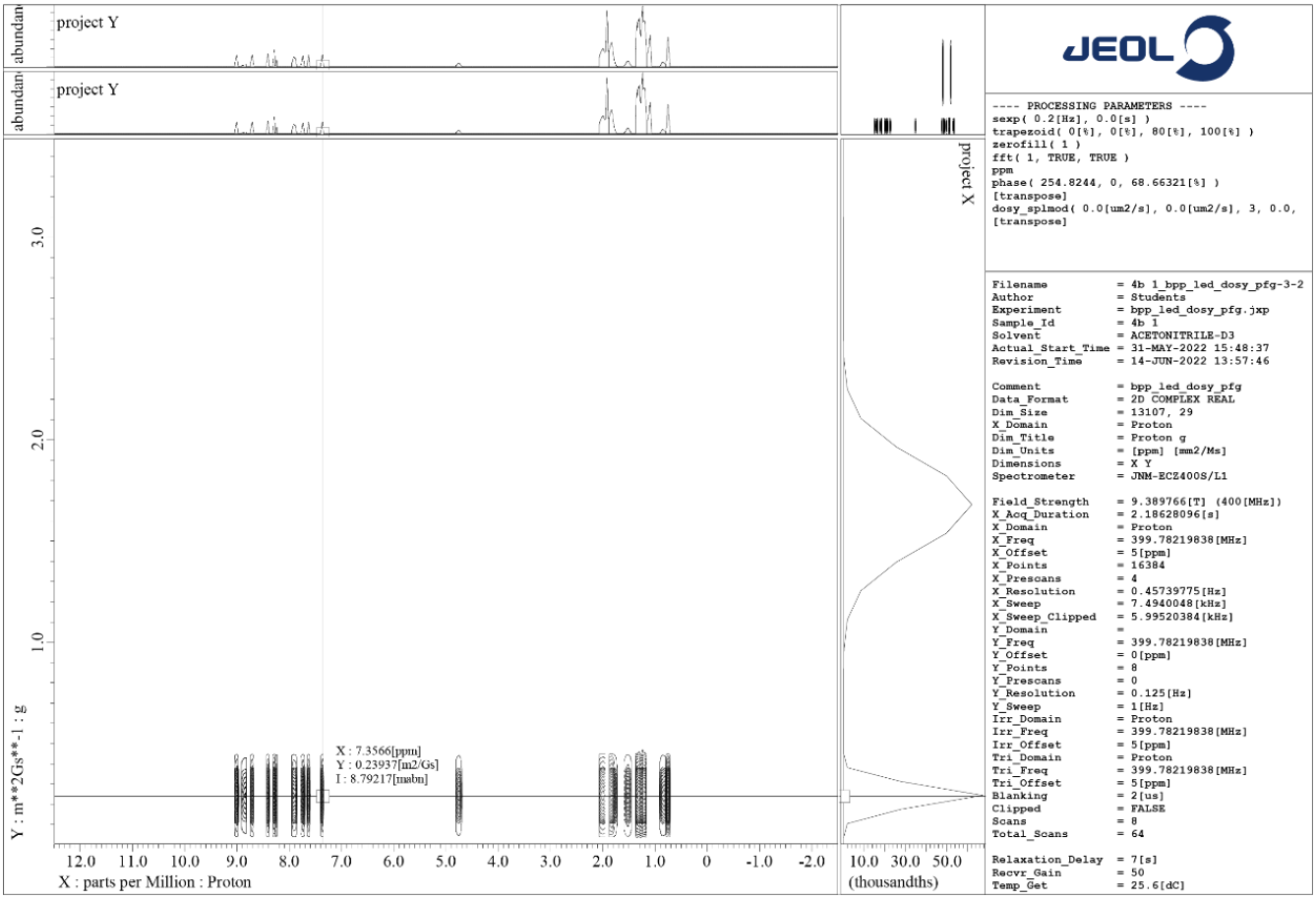

Figure S12. 2D ^{1}H DOSY spectra (400 MHz, CD_3CN, 295 K) recorded for metallacycle **4b.**

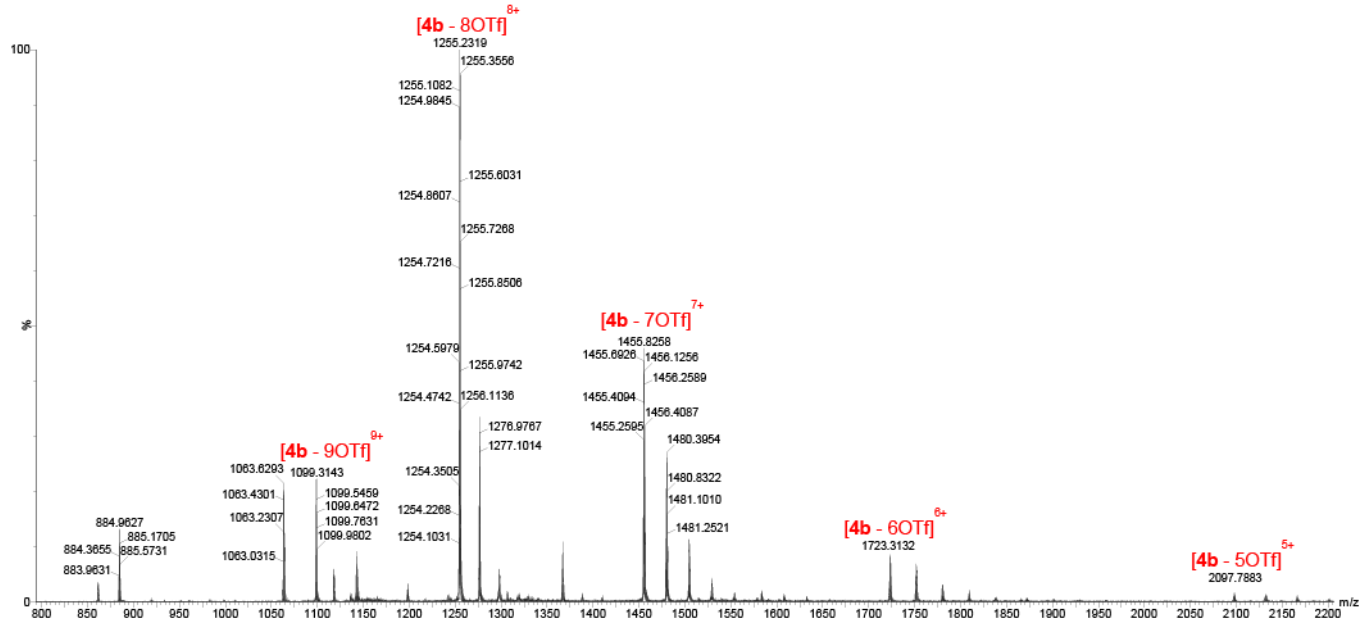

Figure S13. ESI-TOF-MS spectrum of **4b.**

2.8 Self-assembly of metallacage ***4c***

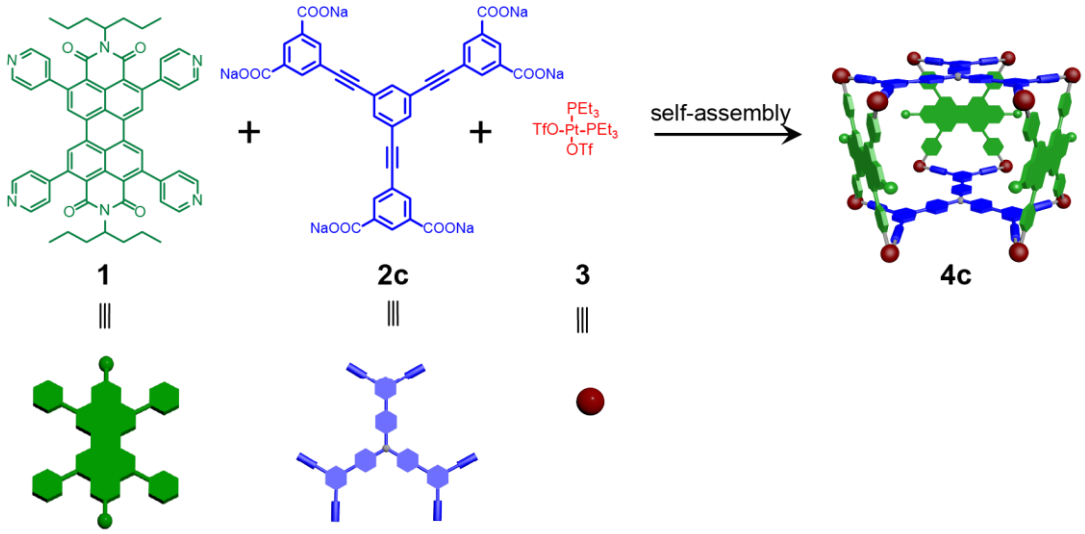

1 (20.00 mg, 22.34 μmol), **2c** (11.54 mg, 14.90μmol) and **3** (65.20 mg, 89.38 μmol) were mixed in a 1:1:4 molar ratio and dissolved in acetone/water (20 mL, 4:1, *v/v*). The whole reaction mixture was heated at 50℃ for 12 hours and then cooled to room temperature. The solvent was removed by nitrogen flow. The residue was redissolved in CH_3CN (1.0 mL) and filtered, and then, ethyl ether (4 mL) was added to give a precipitate, which was collected by centrifugation to give metallacage **4c** (91.2 mg, 92%) as a red solid.^{1}H NMR (600 MHz, CD_3CN, 295 K) δ 9.03–8.94 (m, 12H), 8.73 (dd, J = 5.3, 2.5 Hz, 12H), 8.36 (s, 12H), 8.24 (s, 6H), 8.13 (d, J = 1.5 Hz, 12H), 7.70 (s, 6H), 7.57 (d, J = 5.3 Hz, 12H), 7.43 (d, J = 5.5 Hz, 13H), 4.81–4.68 (m, 12H), 0.76 (t, J = 7.3 Hz, 36H).^{31}P{^{1}H} NMR (243 MHz, CD_3CN, 295 K): 5.27 ppm (d, $^{2}J_{P\text{-}P}$ =19.44 Hz, ^{195}Pt satellites, $^{1}J_{Pt\text{-}P}$ = 1750 Hz), -0.26 ppm (d, $^{2}J_{P\text{-}P}$ =19.44 Hz, ^{195}Pt satellites, $^{1}J_{Pt\text{-}P}$ = 1750 Hz). ESI-TOF-MS: *m/z* 1064.4125 [**4c** – 9OTf]$^{9+}$, 1216.3335 [**4c** – 8OTf]$^{8+}$, 1411.2483 [**4c** – 7OTf]$^{7+}$, 1671.1079 [**4c** – 6OTf]$^{6+}$and 2035.5333 [**4c** – 5OTf]$^{5+}$.

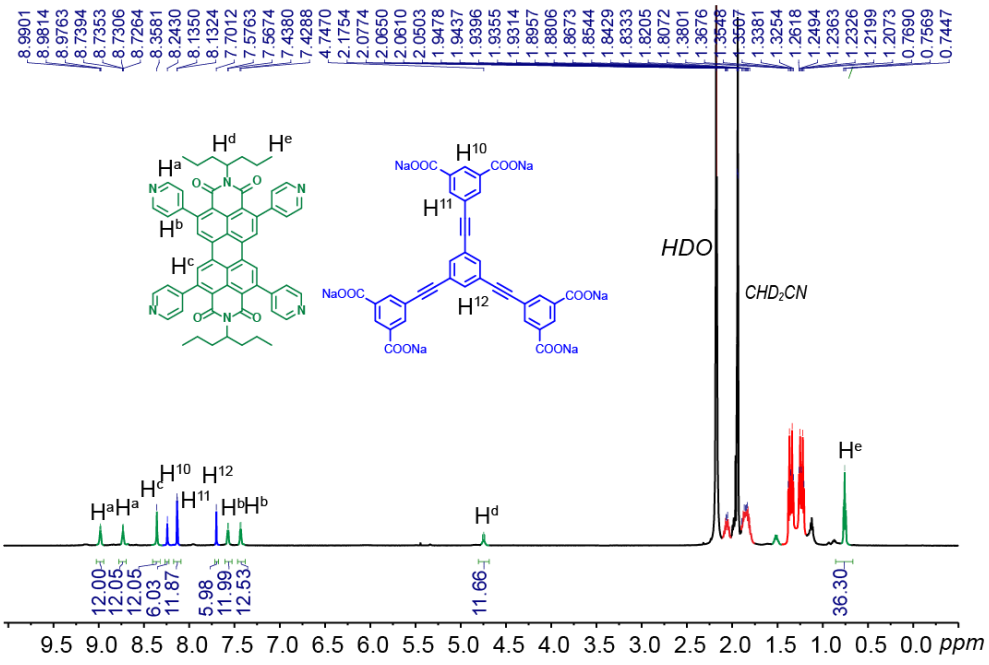

Figure S14. ^{1}H NMR spectrum (600 MHz, CD_3CN, 295 K) recorded for **4c**.

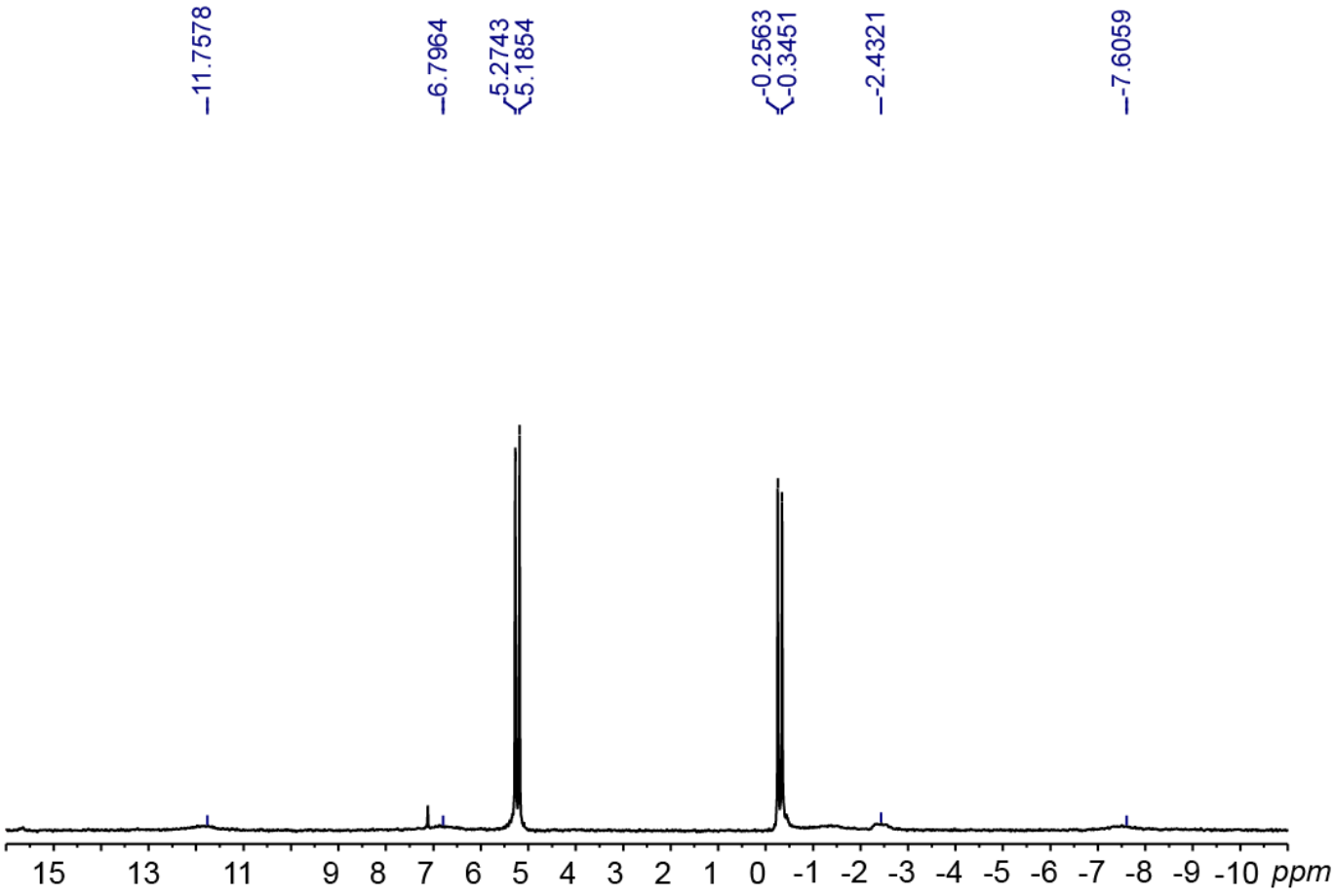

Figure S15. $^{31}P\{^{1}H\}$ NMR spectrum (162 MHz, CD_3CN, 295 K) recorded for **4c**.

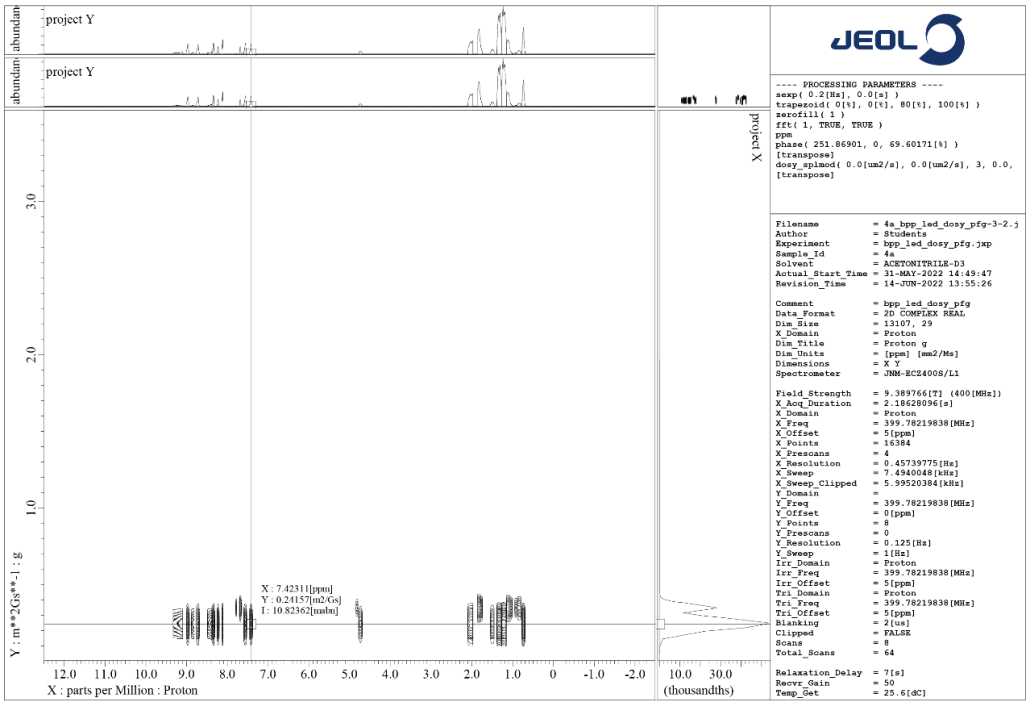

Figure S16. 2D ^{1}H DOSY spectra (400 MHz, CD_3CN, 295 K) recorded for metallacycle **4c**.

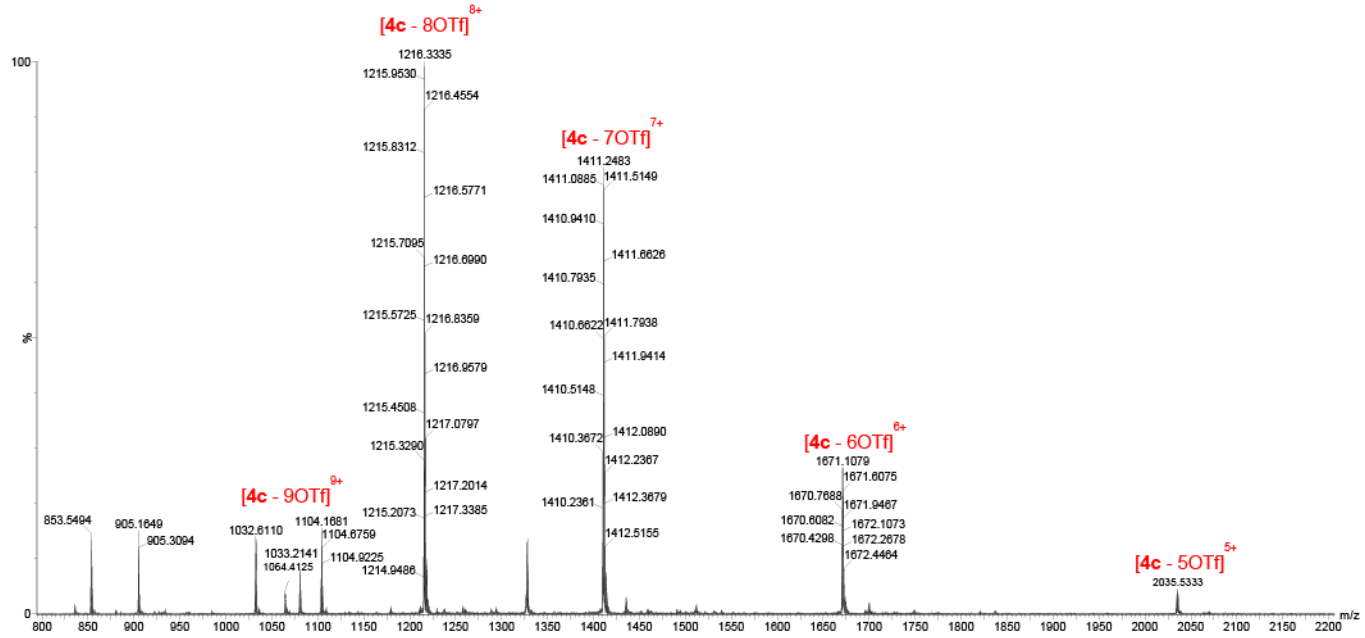

Figure S17. ESI-TOF-MS spectrum of **4c.**

*3. Crystallographic data and refinement details for metallacages **4a** and **4c***

Table S1. Crystallographic data and refinement details for metallacages **4a** and **4c**.

Compound	**4a**
Empirical formula	C_{402} H_{546} N_{20} O_{36} P_{24} Pt_{12}
Fw	9318.92
Crystal system	hexagonal
Space group	*P 63*
a /Å	40.1356(18)
b /Å	40.1356(18)
c /Å	28.0718(13)
α /°	90
β /°	90
γ /°	120
V /Å^3	39162(4)
Z	2
D_{calc}/g cm^{-3}	0.790
F (000)	9364.0
μ /mm^{-1}	3.158
θ max	54.138
Reflns [$I > 2\sigma(I)$]	48131
R_1; wR_2 [$I > 2\sigma(I)$]	0.0633; 0.1891

Compound	**4c**
Empirical formula	$C_{390}\ H_{534}\ N_{18}\ O_{36}\ P_{24}\ Pt_{12}$
Fw	9134.68
Crystal system	hexagonal
Space group	*P 63*
a /Å	39.8460(10)
b /Å	39.8460(10)
c /Å	28.1489(13)
α /°	90
β /°	90
γ /°	120
V /Å^3	38704(3)
Z	2
D_{calc}/g cm^{-3}	0.784
F (000)	9168.0
μ /mm^{-1}	4.668
θ max	61.127
Reflns [$I > 2\sigma(I)$]	29120
R_1; wR_2 [$I > 2\sigma(I)$]	0.0857; 0.2193

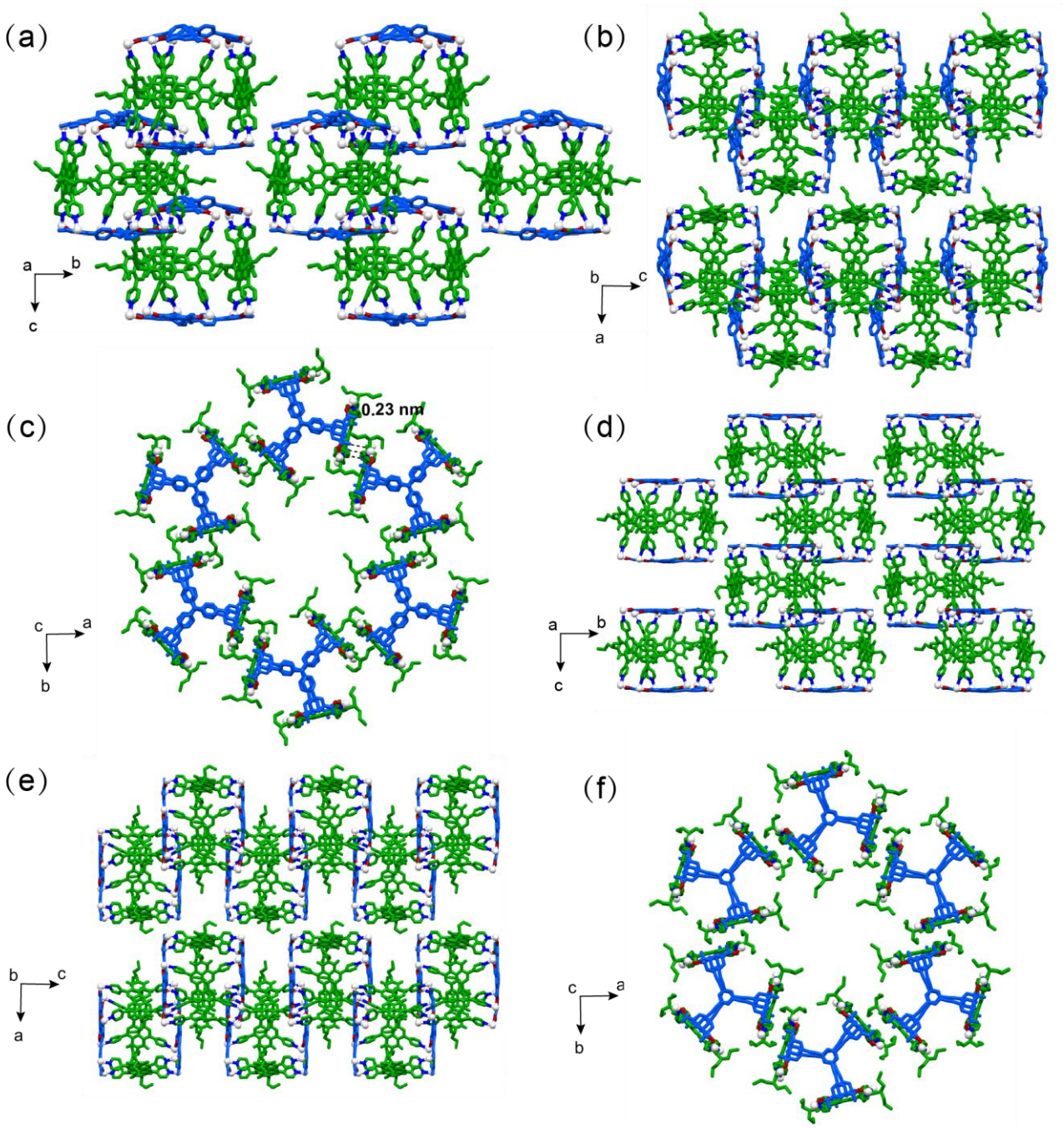

Figure ***S18.*** Crystal packing model of metallacage **4a** viewed from (a) a axis, (b) b axis, and (c) c axis. Crystal packing model of metallacage **4c** viewed from (d) a axis, (e) b axis, and (f) c axis. Hydrogen atoms, counterions, triethylphosphine units and solvent molecules are omitted for clarity.

*4. Measurements of absolute fluorescence quantum yields for **1**, **4a**, **4b**, and **4c***

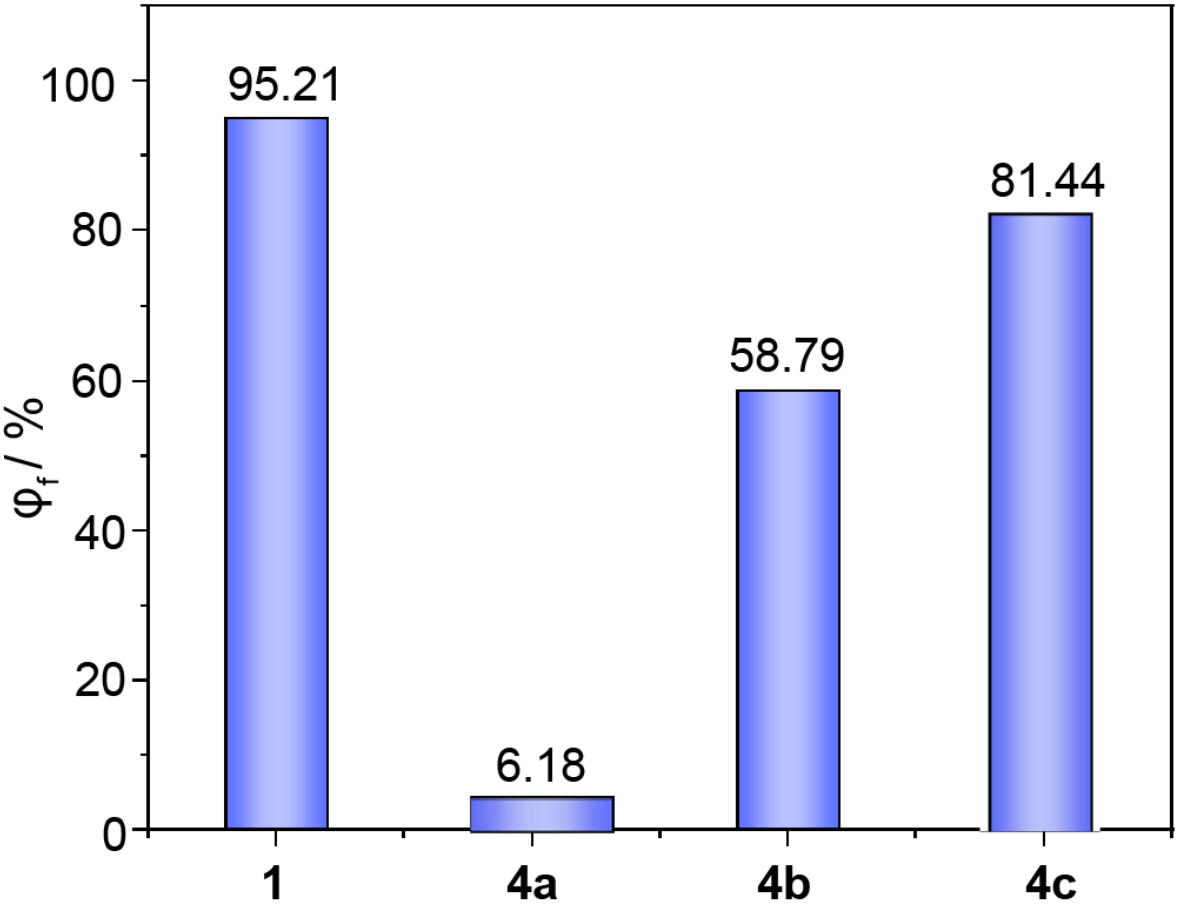

Figure S19. Absolute fluorescence quantum yields of **1** and **4a**–**4c** in CH_3CN (λ_{ex} = 365 nm, c = 10.0 μM, 295 K)

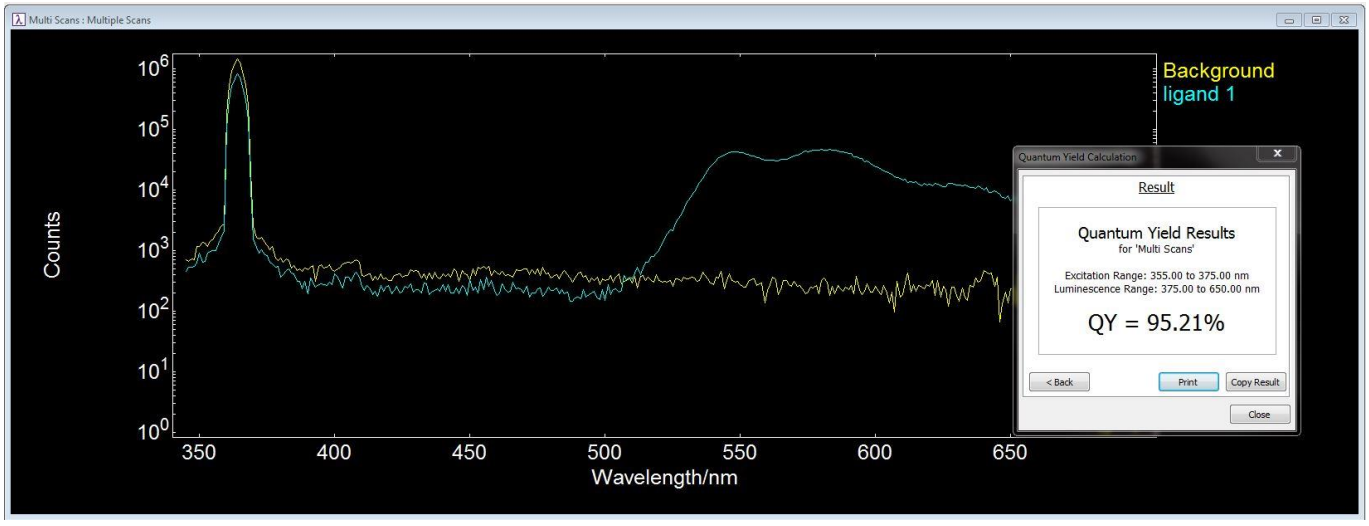

Figure S20. Absolute fluorescence quantum yield of ligand **1** in CH_3CN.

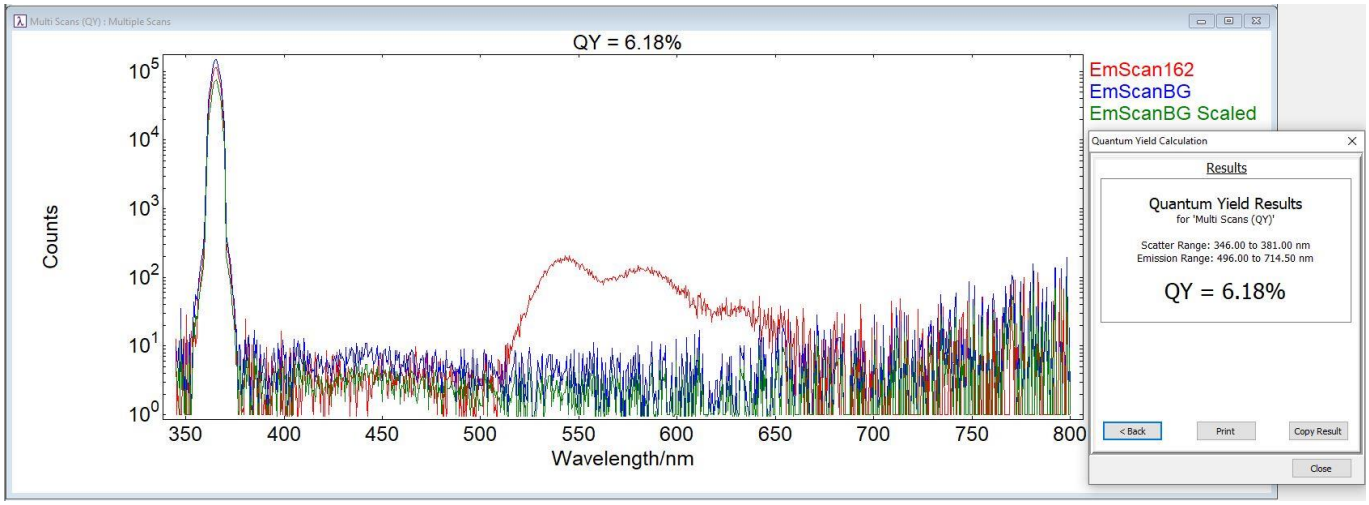

Figure S21. Absolute fluorescence quantum yield of metallacage **4a** in CH_3CN.

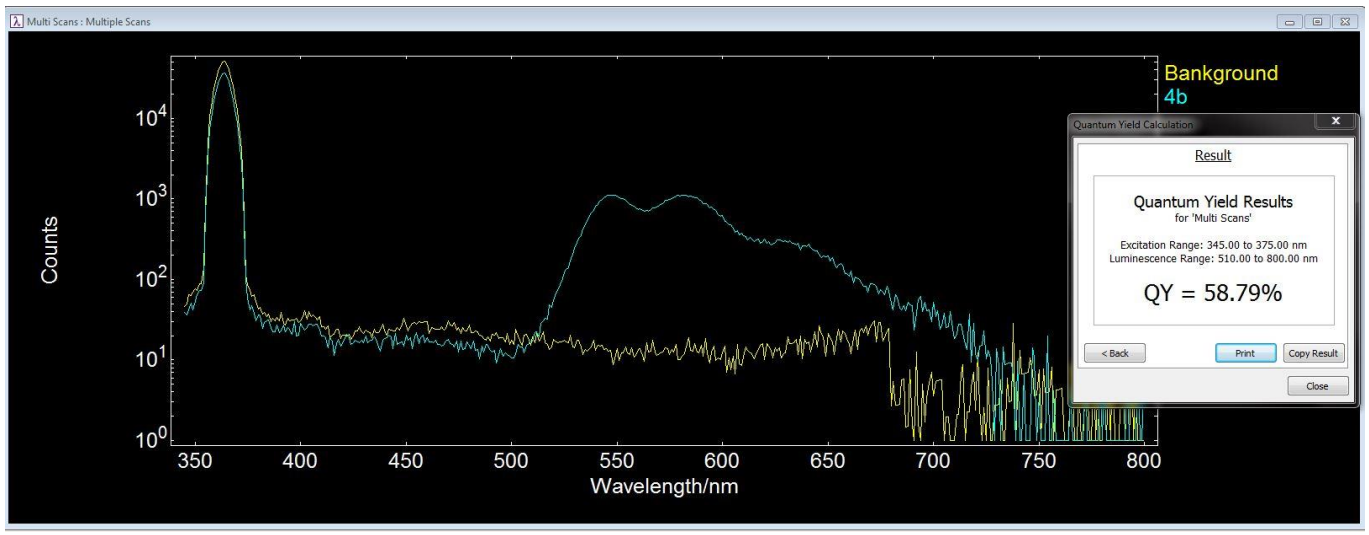

Figure S22. Absolute fluorescence quantum yield of metallacage **4b** in CH_3CN.

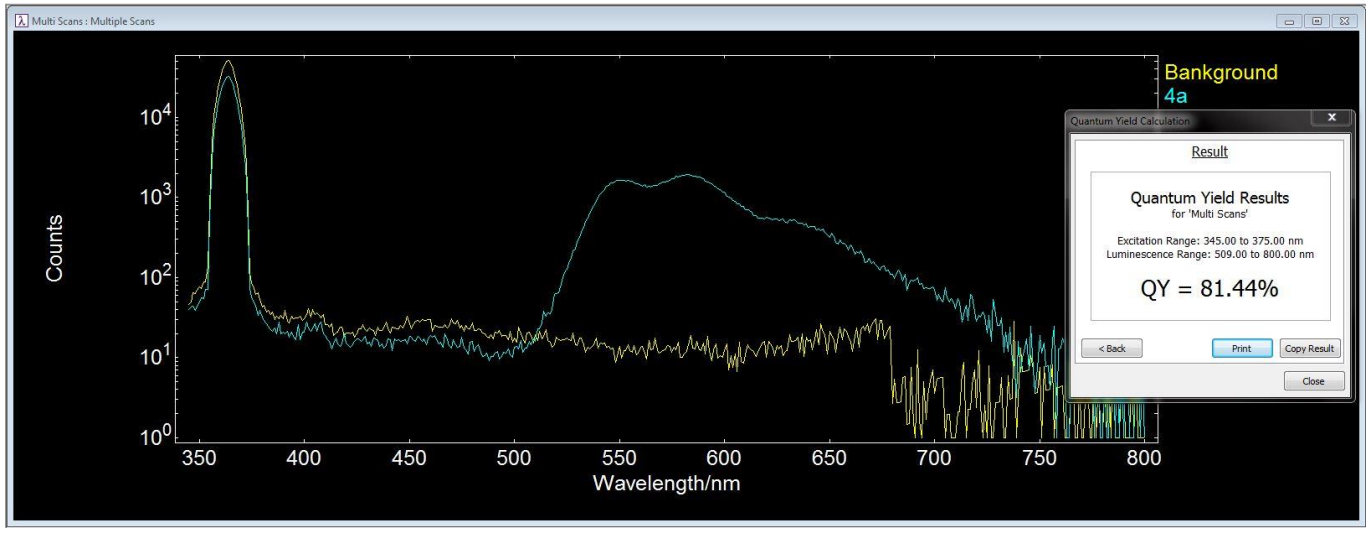

Figure S23. Absolute fluorescence quantum yield of metallacage **4c** in CH_3CN.

*5. Fluorescence decay traces and lifetime for **1**, **4a**, **4b**, and **4c***

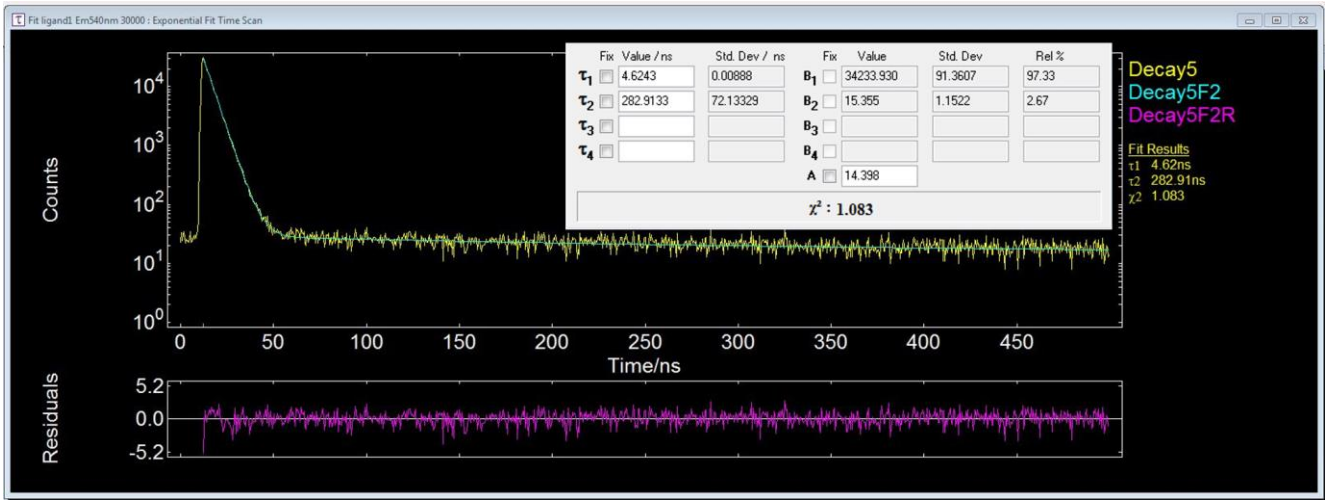

Figure S24. Fitting spectra of fluorescence decays of **1**, monitored at 540 nm with an excitation wavelength of 375 nm.

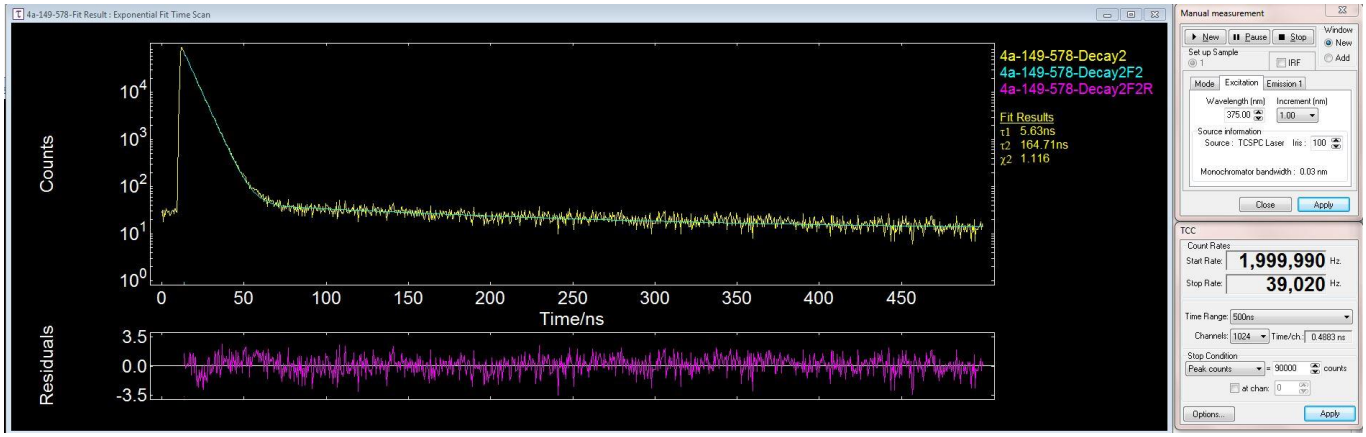

Figure S25 Fitting spectra of fluorescence decays of **1**, monitored at 578 nm with an excitation wavelength of 375 nm.

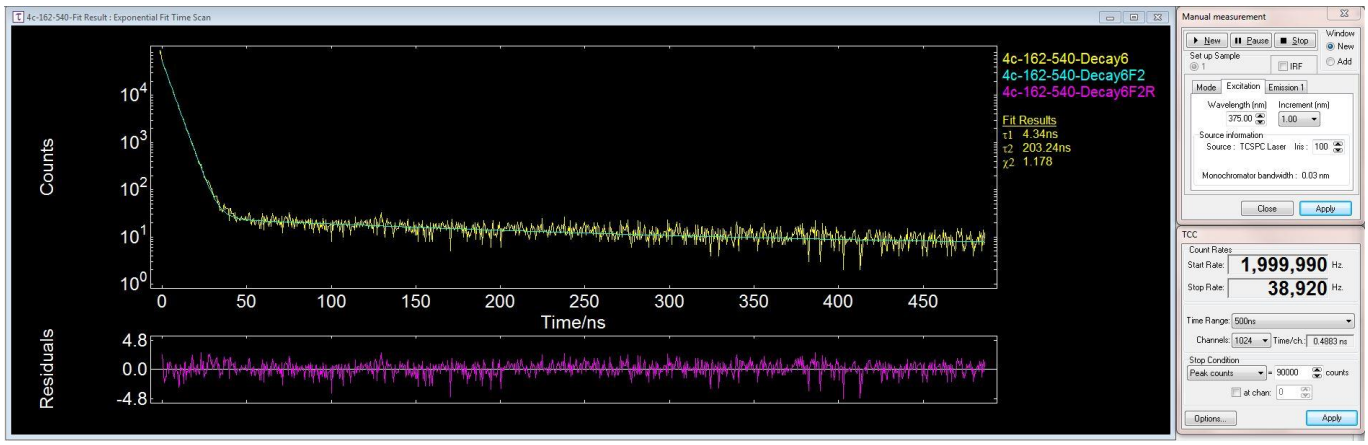

Figure S26. Fitting spectra of fluorescence decays of **4a**, monitored at 540 nm with an excitation wavelength of 375 nm.

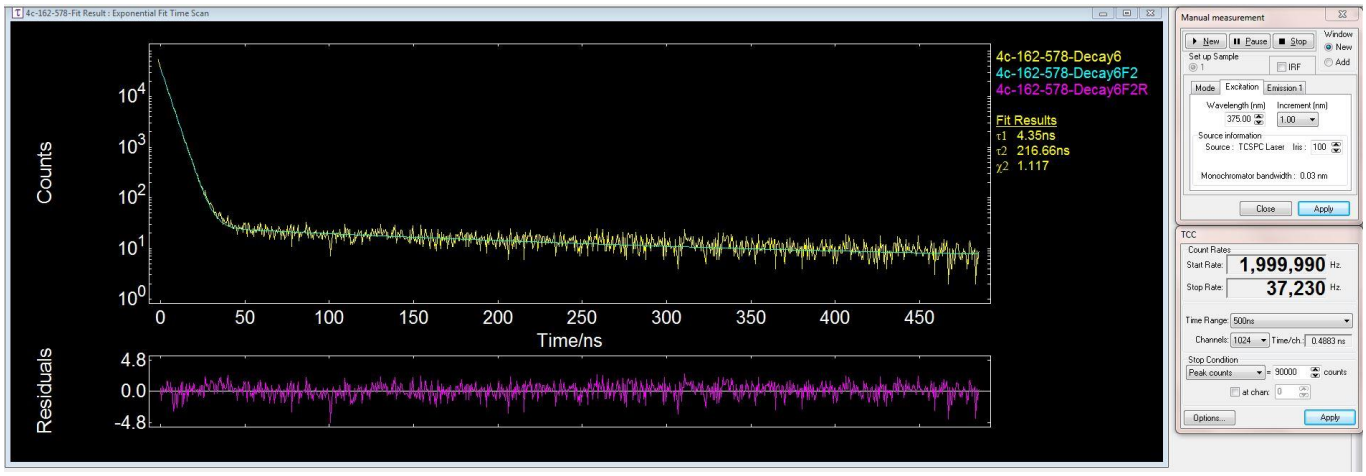

Figure S27. Fitting spectra of fluorescence decays of **4a**, monitored at 578 nm with an excitation wavelength of 375 nm.

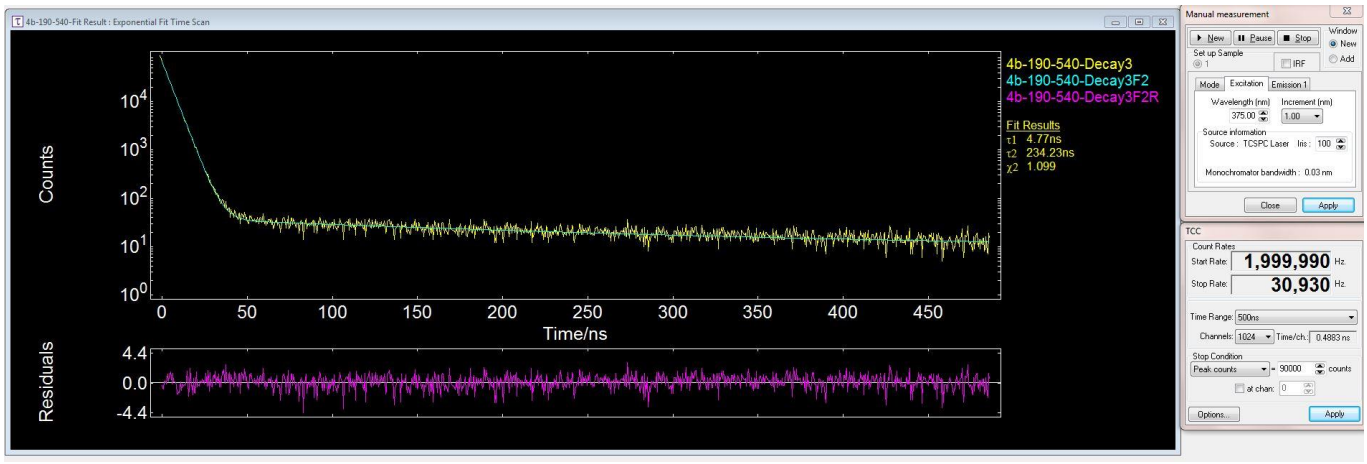

Figure S28. Fitting spectra of fluorescence decays of **4b**, monitored at 540 nm with an excitation wavelength of 375 nm.

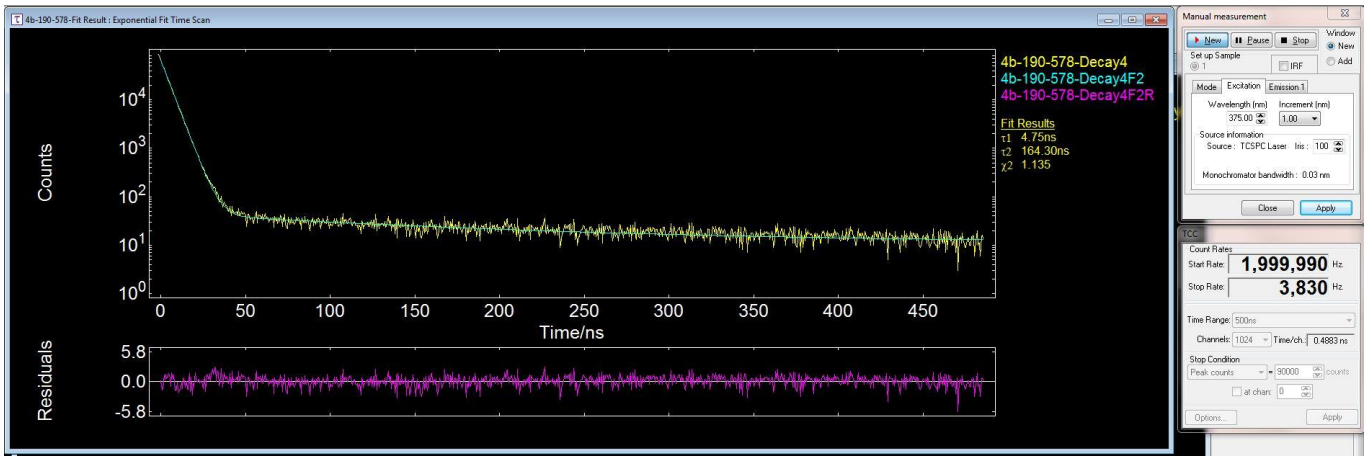

Figure S29. Fitting spectra of fluorescence decays of **4b**, monitored at 578 nm with an excitation wavelength of 375 nm.

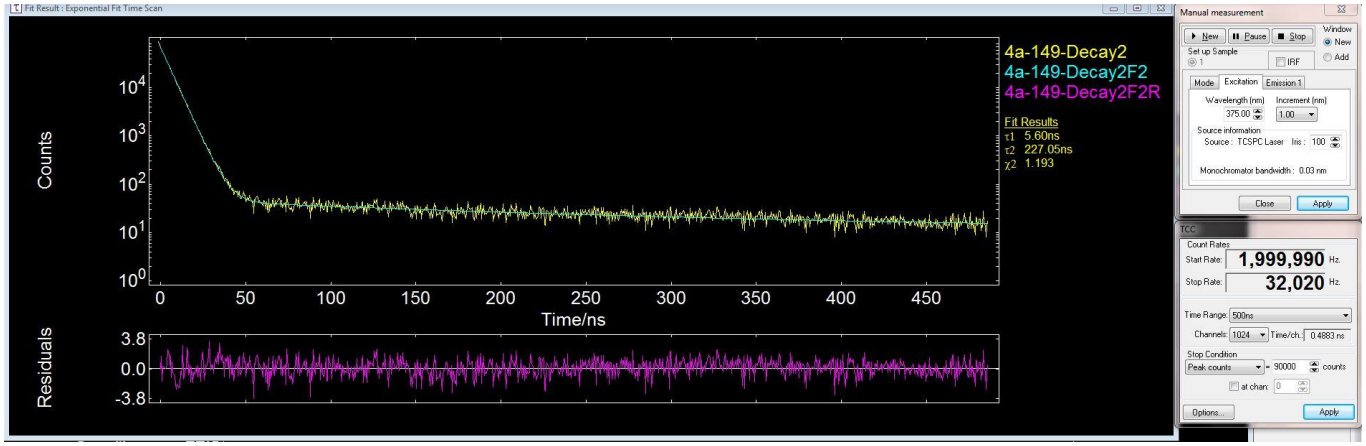

Figure S30. Fitting spectra of fluorescence decays of **4c**, monitored at 540 nm with an excitation wavelength of 375 nm.

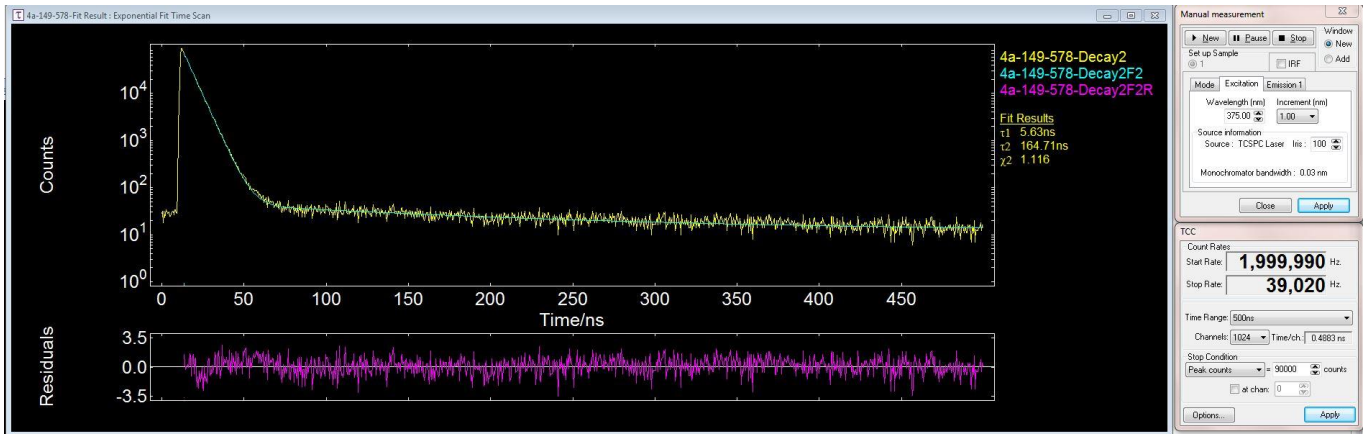

Figure S31. Fitting spectra of fluorescence decays of **4c**, monitored at 578 nm with an excitation wavelength of 375 nm.

6.Host-guest complexation study

6.1 ^{1}H NMR study of complexes

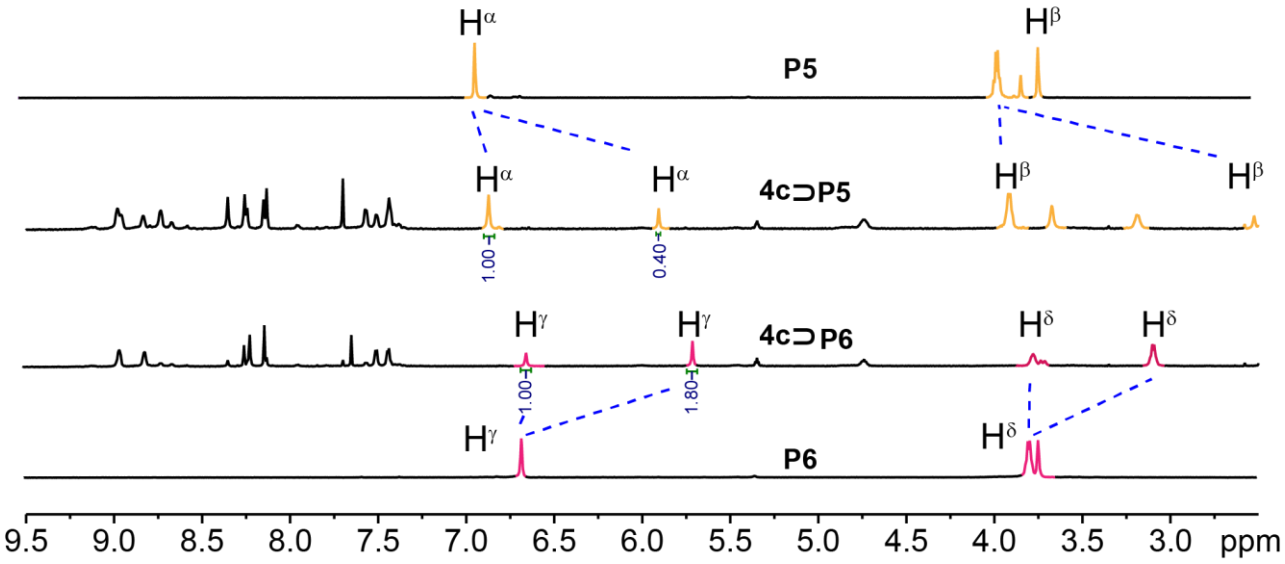

Figure S32. Partial ^{1}H NMR spectra (400 MHz, CD_3CN, 295 K) of **P5**, **4c⊃P5**, **4c**, **4c⊃P6** and **P6**.

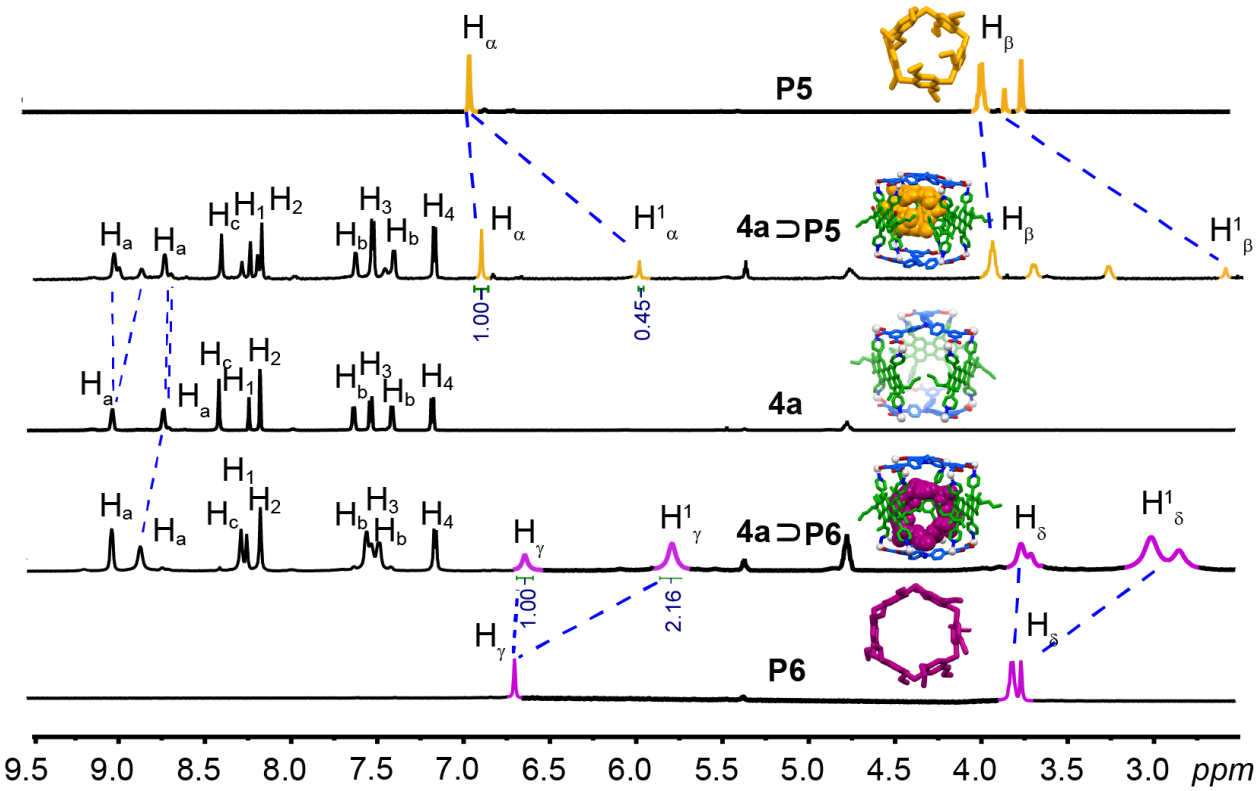

Figure S33. Partial ^{1}H NMR spectra (400 MHz, CD_3CN, 295 K) of pillararene **P5**, **4a⊃P5, 4b, 4a⊃P6** and **P6.**

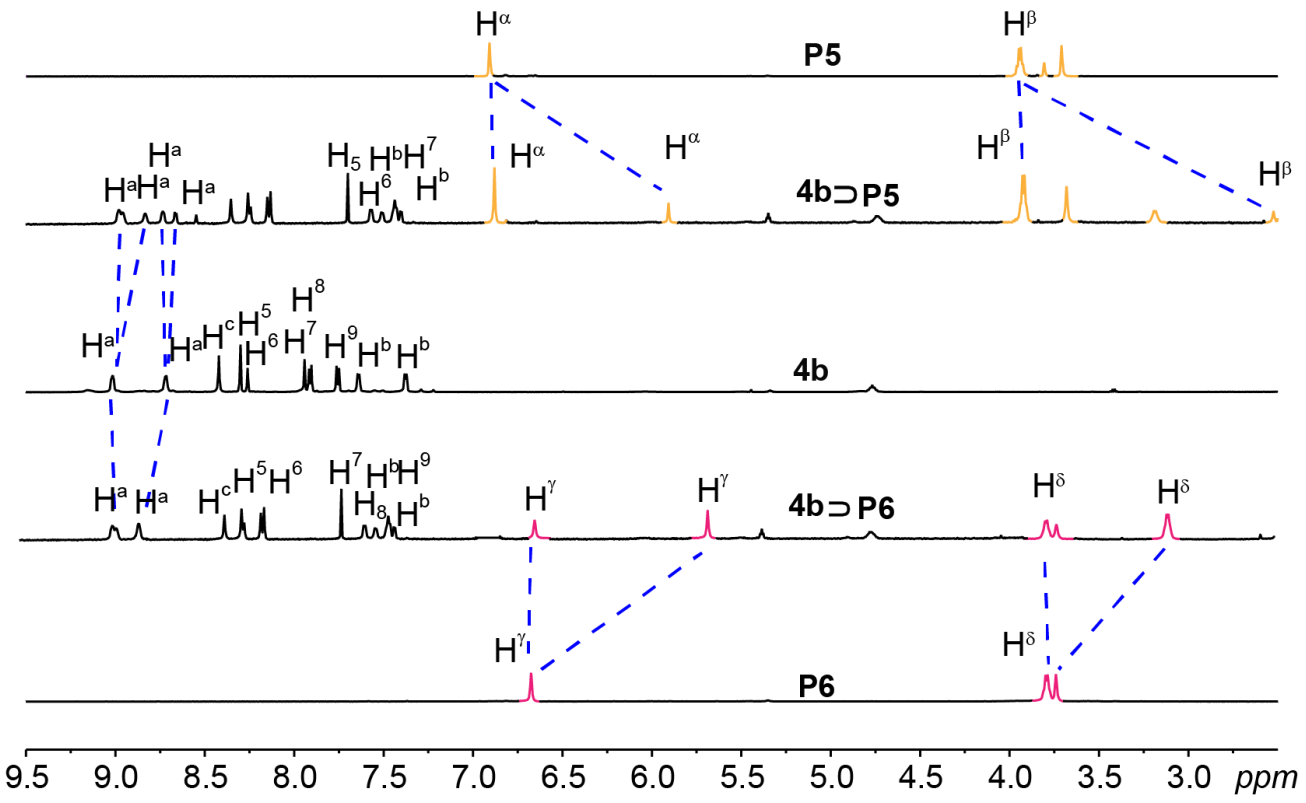

Figure S34. Partial ^{1}H NMR spectra (400 MHz, CD_3CN, 295 K) of **P5**, **4b⊃P5, 4b, 4b⊃P6** and **P6.**

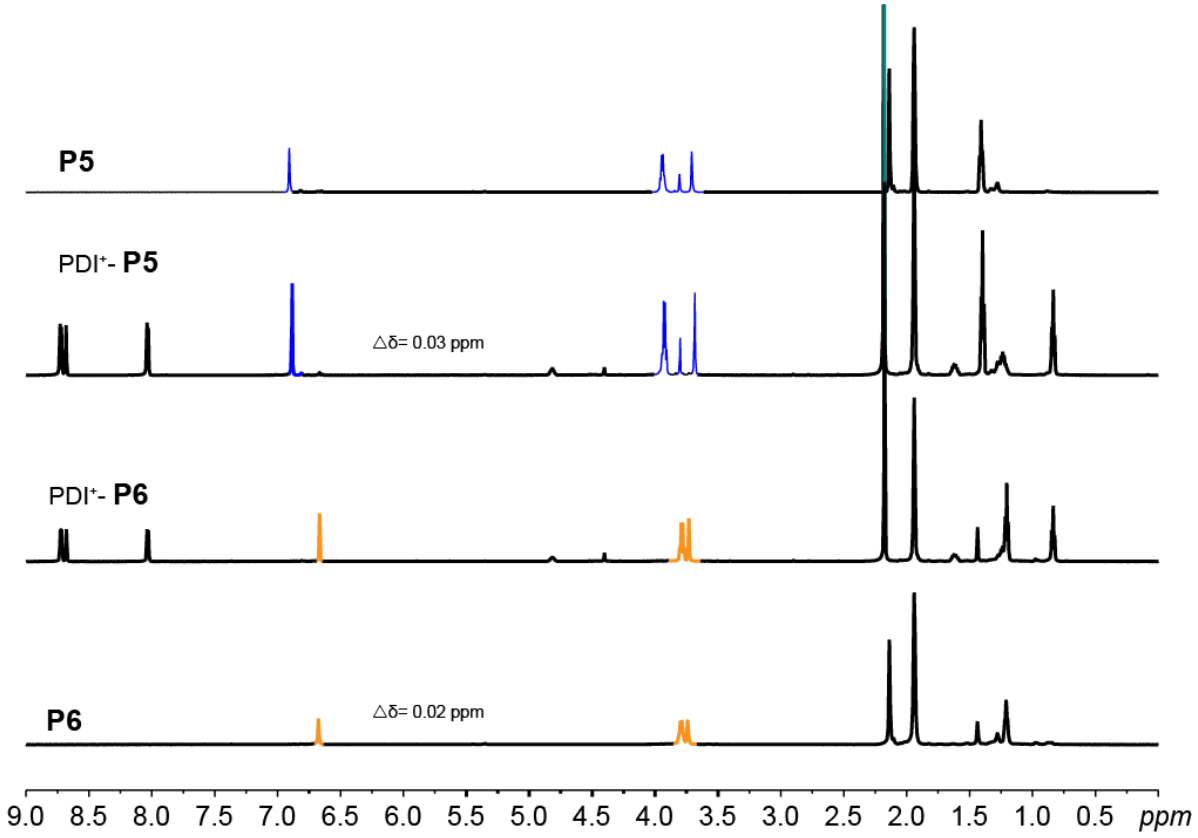

Figure S35. Partial ^{1}H NMR spectra (400 MHz, CD_3CN, 295 K) of the mixture of PDI and Pillararene. PDI : Pillararene = 1:1**.**

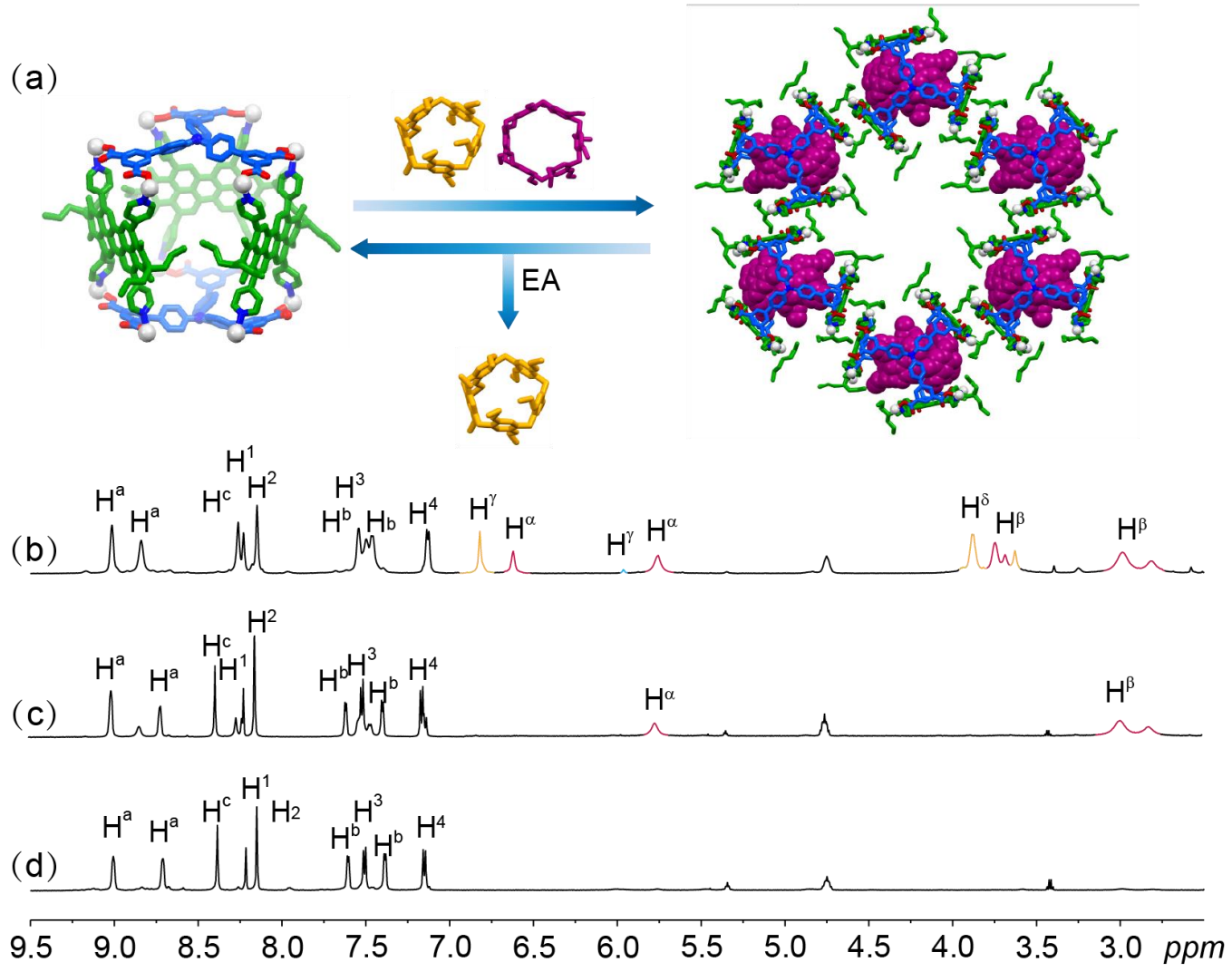

Figure S36. (a) Crystal structure of the complexation between metallacage **4a** and pillararenes. (b) Partial ^{1}H NMR spectra (400 MHz, CD_3CN, 295 K) of the combination of selectivity between **4a** and pillararene. (c) Partial ^{1}H NMR spectra (400 MHz, CD_3CN, 295 K) of the complex after being washed once with ethyl acetate (EA). (d) Partial ^{1}H NMR spectra (400 MHz, CD_3CN, 295 K) of the complex after being washed twice with EA.

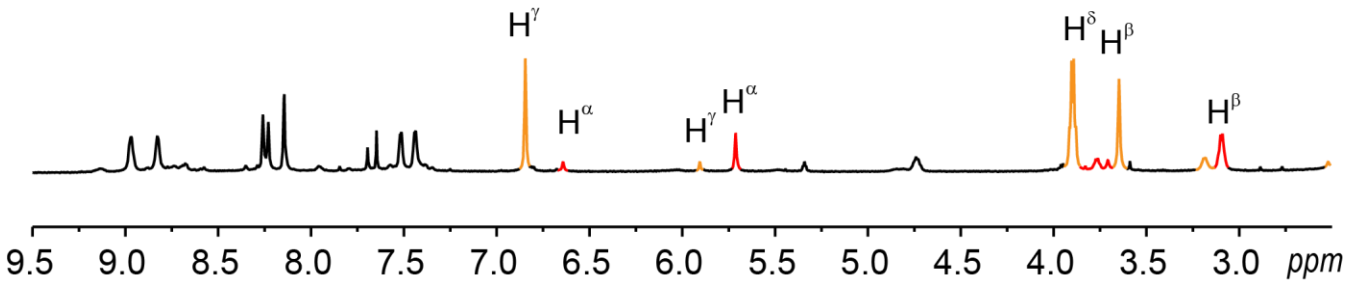

Figure S37. (a) Partial ^{1}H NMR spectra (400 MHz, CD_3CN, 295 K) of the combination of selectivity between **4c** and pillararene.

6.2 Mass spectra study of complexes

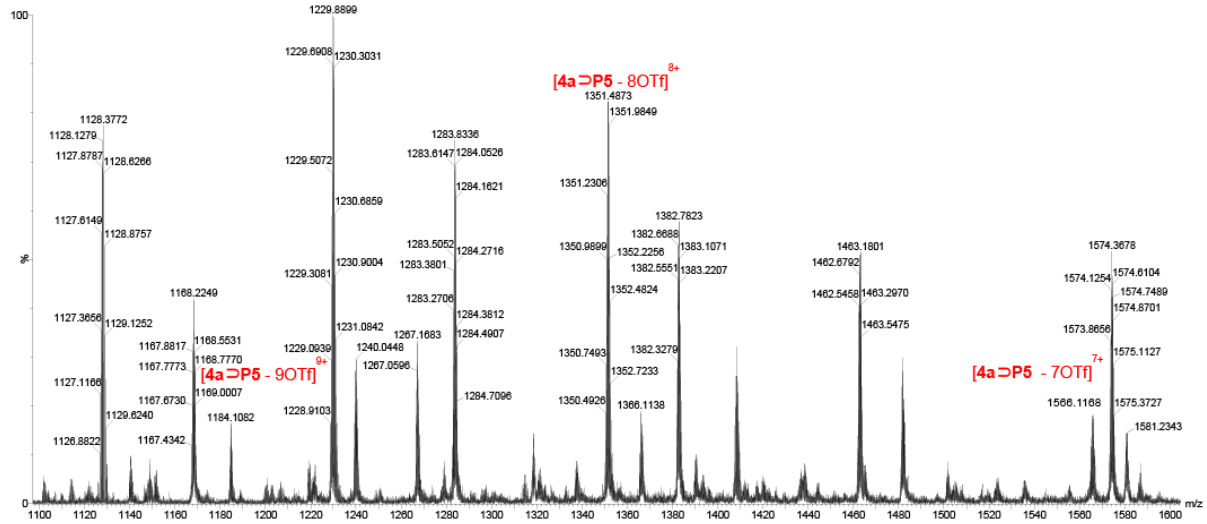

Figure S38. ESI-TOF-MS spectra of **4a⊃P5**.

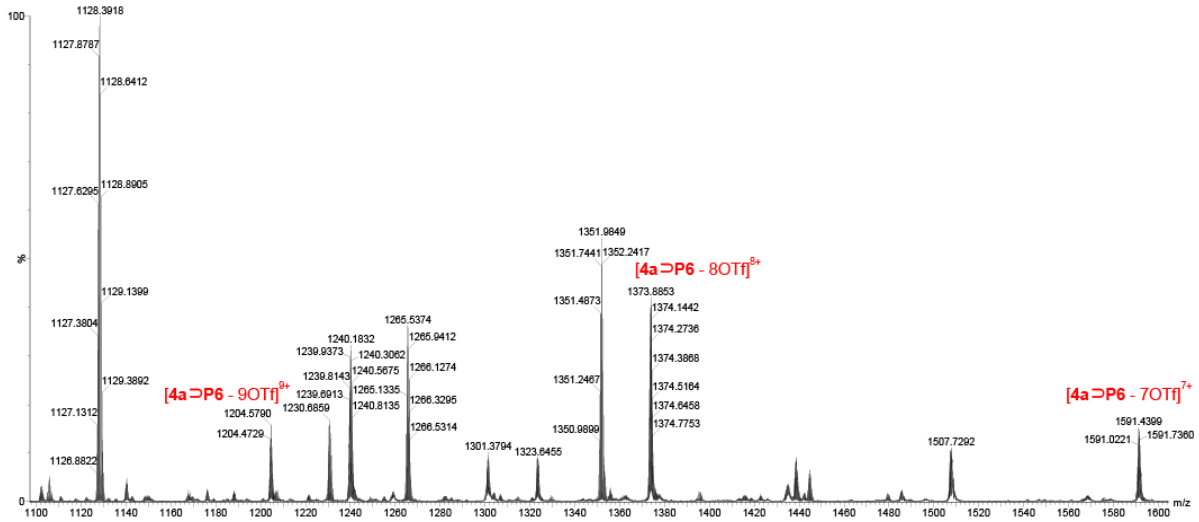

Figure S39. ESI-TOF-MS spectra of **4a⊃P6**.

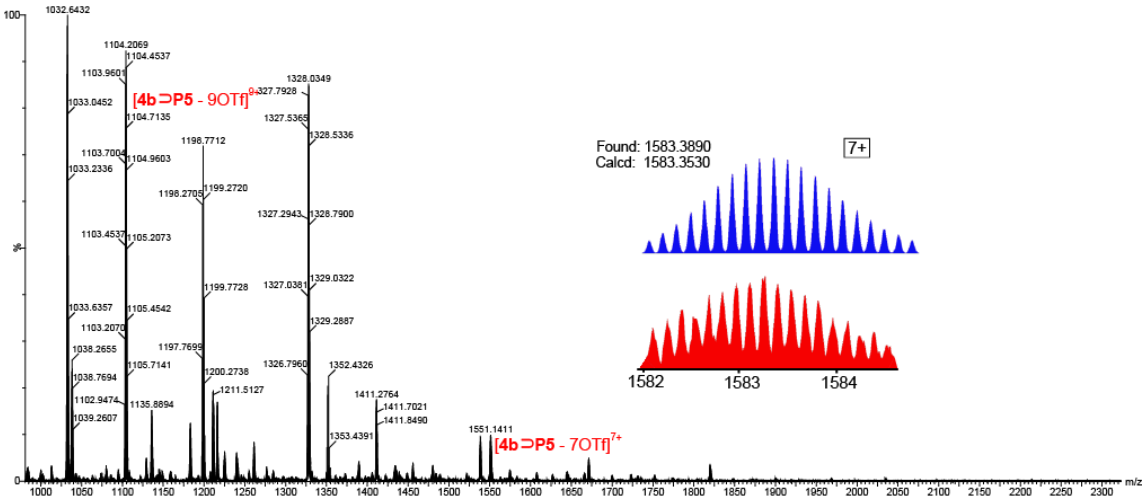

Figure S40. ESI-TOF-MS spectra of **4b⊃P5**.

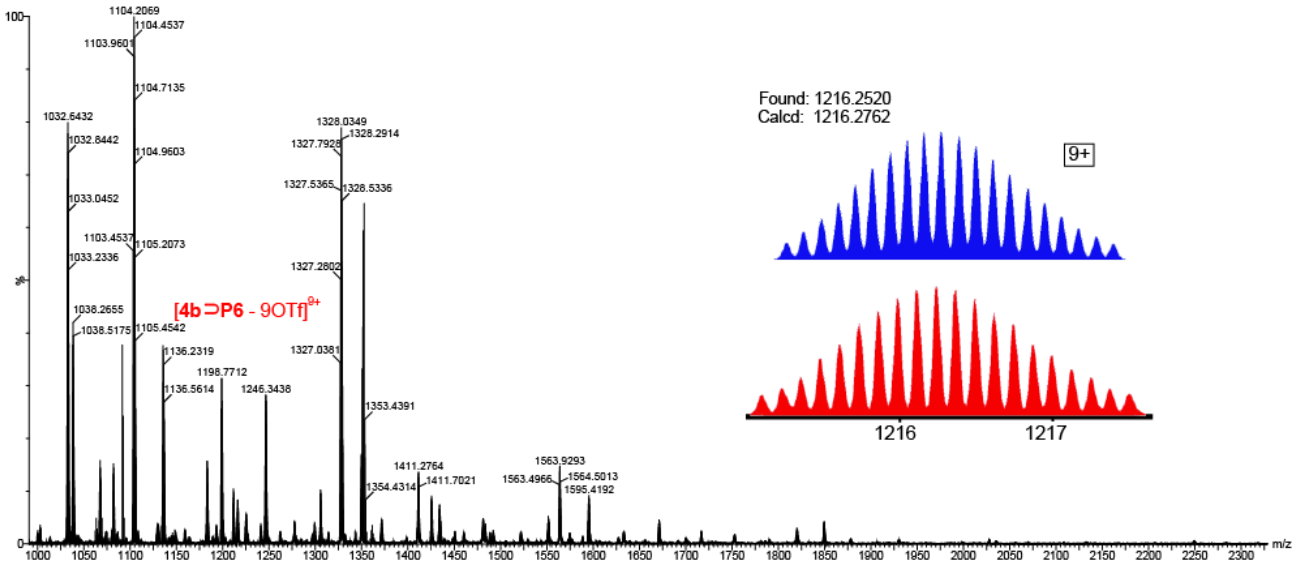

Figure S41. ESI-TOF-MS spectra of **4b⊃P6**.

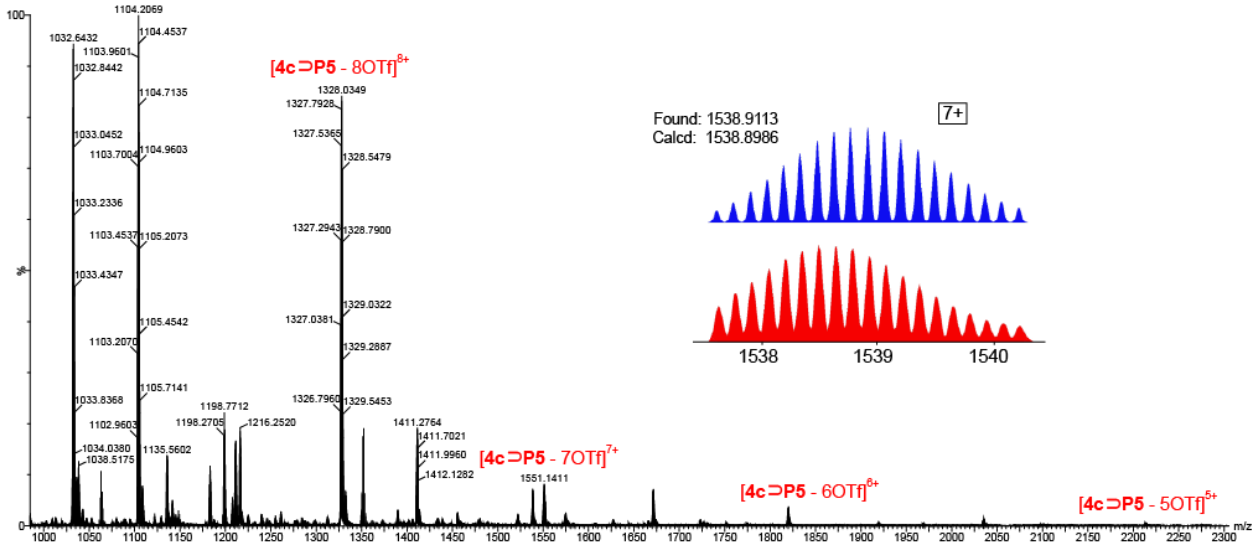

Figure S42. ESI-TOF-MS spectra of **4c⊃P5**.

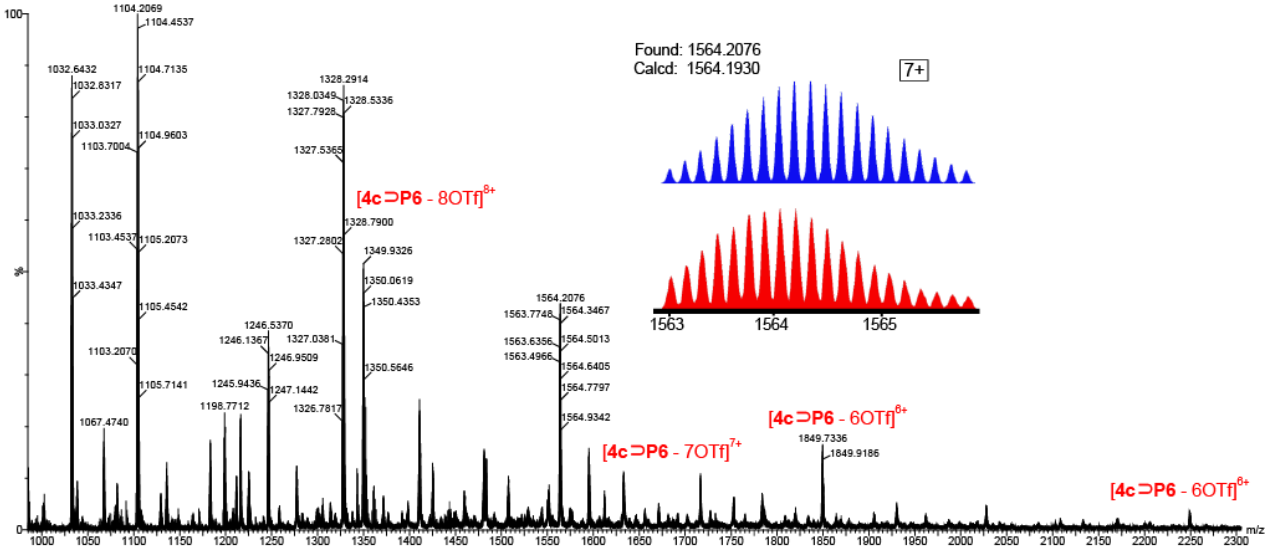

Figure S43. ESI-TOF-MS spectra of **4c⊃P6**.

*6.3 Crystallographic structure and data for **4a⊃P5**, **4a⊃P6**, and **4c⊃P5***

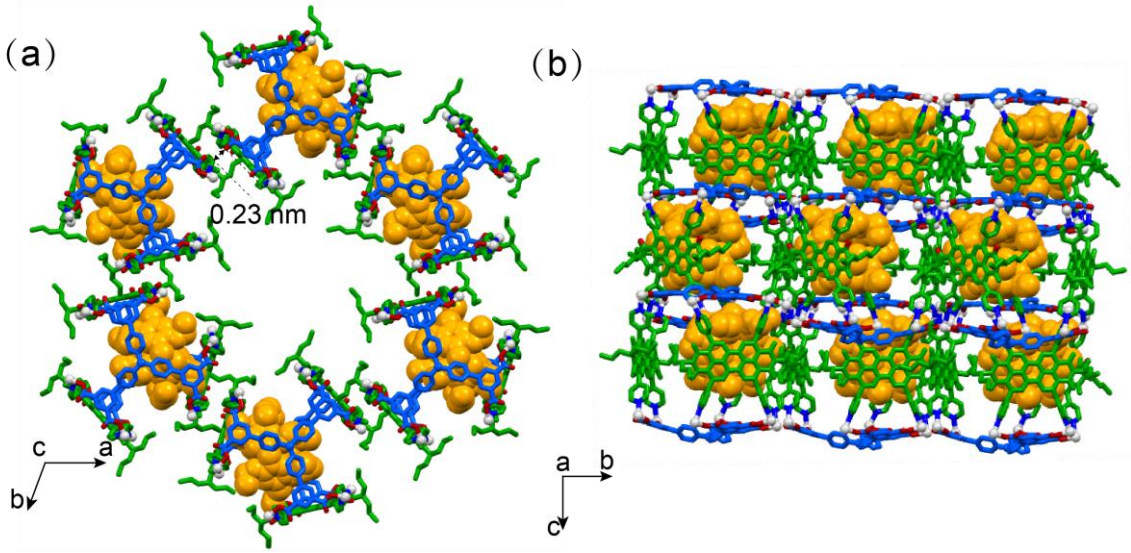

Figure S44. Crystal packing model of **4a⊃P5**

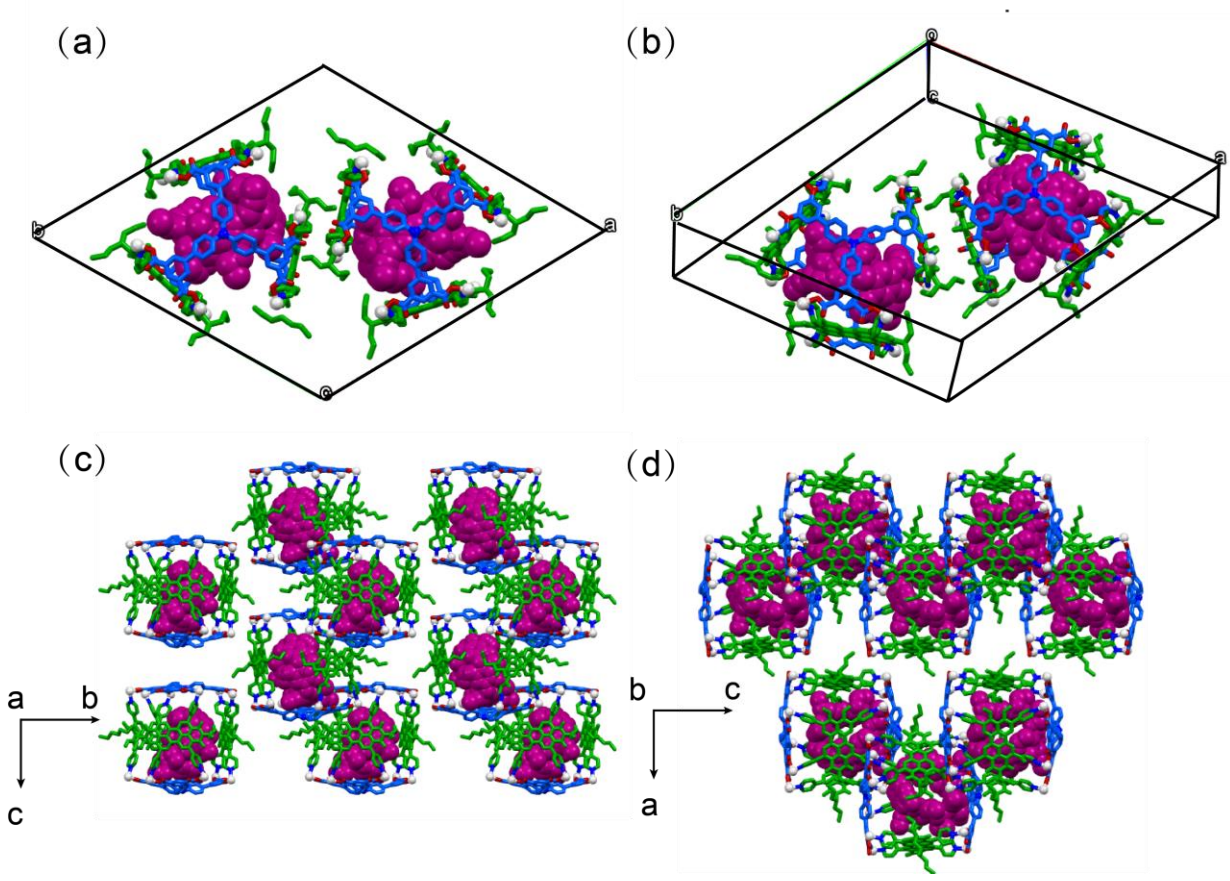

Figure S45. Crystal packing model of **4a⊃P6**

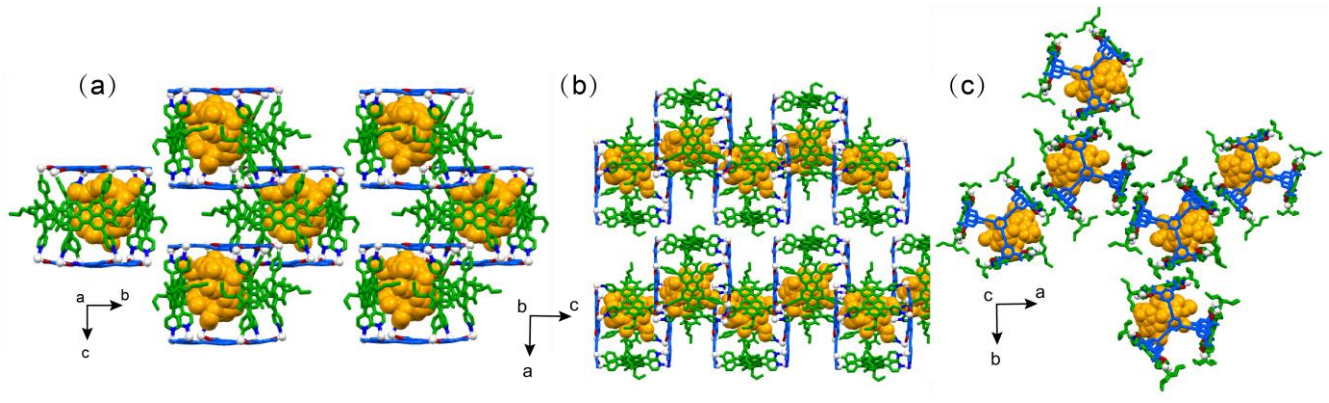

Figure S46. Crystal packing model of **4c⊃P5**

Table S2. Crystallographic data and refinement details for **4a⊃P5, 4a⊃P6** and **4c⊃P5**.

Compound	**4a⊃P5**
Empirical formula	$C_{453}H_{604}F_{31}N_{20}O_{75}P_{24}Pt_{12}S_{10}$
Fw	11558.53
Crystal system	hexagonal
Space group	*P* 63
a /Å	40.579(11)
b /Å	40.579(11)
c /Å	28.378(9)
α /°	90
β /°	90
γ /°	120
V /Å^3	40468(25)
Z	1
D_{calc}/g cm^{-3}	0.949
F (000)	11629.0
μ /mm^{-1}	3.328
θ max	53.843
Reflns [$I > 2\sigma(I)$]	48184
R_1; wR_2 [$I > 2\sigma(I)$]	0.0615; 0.1893

Compound	**4a⊃P6**
Empirical formula	$C_{459}H_{588}F_{22.50}N_{20}O_{67.50}P_{24}Pt_{12}S_{7.50}$
Fw	11217.77
Crystal system	hexagonal
Space group	*P* 63
a /Å	39.93(9)
b /Å	39.93(9)
c /Å	27.99 (10)
α /°	90
β /°	90
γ /°	120
V /Å^3	38653(2)
Z	2
D_{calc}/g cm^{-3}	0.96
F (000)	11281
μ /mm^{-1}	5.01
θ max	53.75
Reflns [$I > 2\sigma(I)$]	29762
R_1; wR_2 [$I > 2\sigma(I)$]	0.07; 0.20

Compound	**4c⊃P5**
Empirical formula	$C_{431.25}\ H_{586.50}\ N_{18}\ O_{43.50}\ P_{24}\ Pt_{12}$
Fw	9803.01
Crystal system	hexagonal
Space group	*P* 63
a /Å	39.8460(10)
b /Å	39.8460(10)
c /Å	28.1489(13)
α /°	90
β /°	90
γ /°	120
V /Å^3	38704(3)
Z	2
D_{calc}/g cm^{-3}	0.841
F (000)	9888
μ /mm^{-1}	4.699
θ max	0.625
Reflns [$I > 2\sigma(I)$]	0.570,
R_1; wR_2 [$I > 2\sigma(I)$]	0.0949; 0.2405

6.4 UV-Vis study of metallacages and complexes

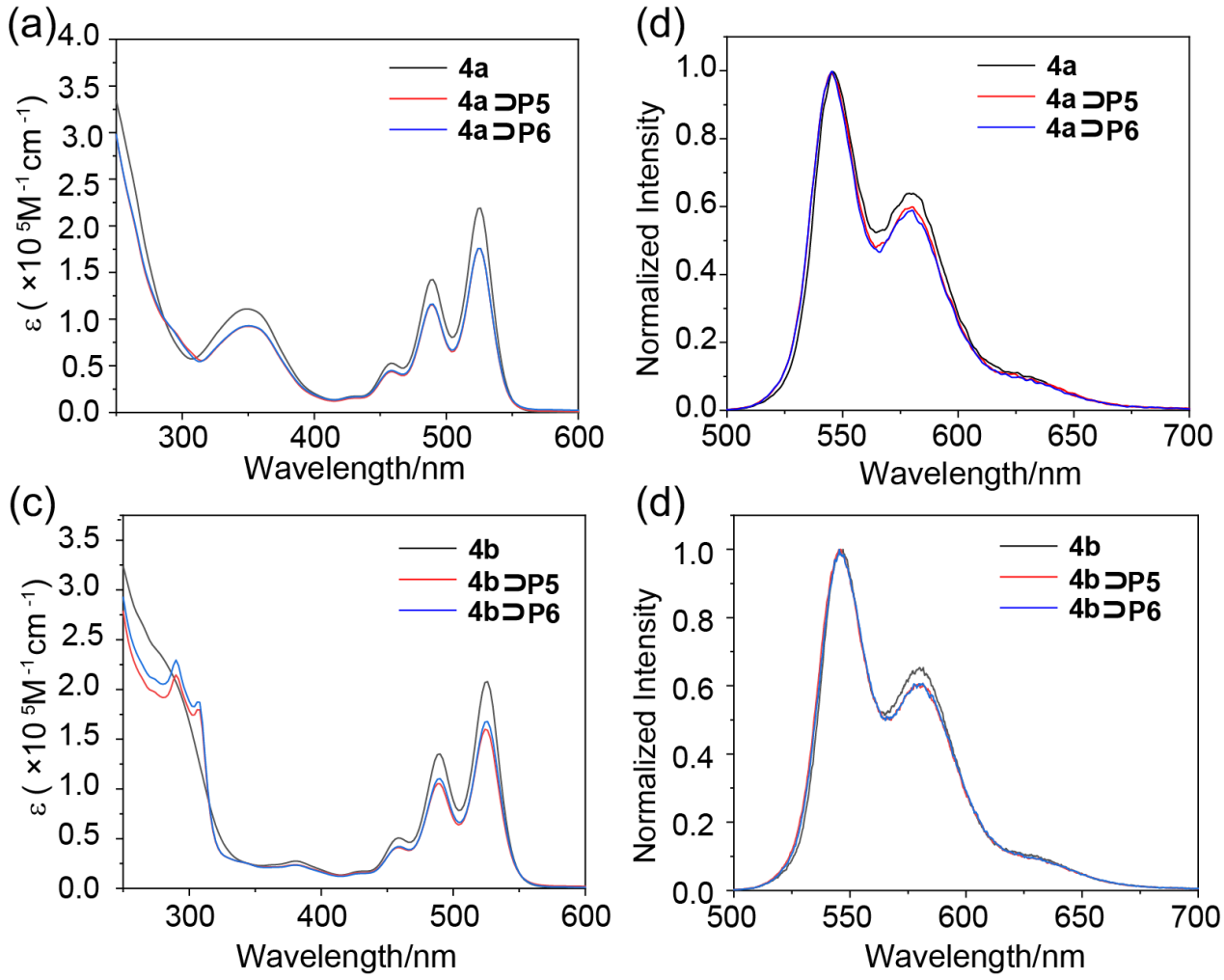

Figure S47. (a) UV–vis absorption and (b) fluorescence spectra of metallacage **4a** and complexes **4a⊃P5** and **4a⊃P6;** (c) UV–vis absorption and (d) fluorescence spectra of metallacage **4b** and complexes **4b⊃P5** and **4b⊃P6** in acetonitrile (λ_{ex} = 365 nm, 10 μM).

6.5 Absolute fluorescence quantum yield study of metallacages and complexes

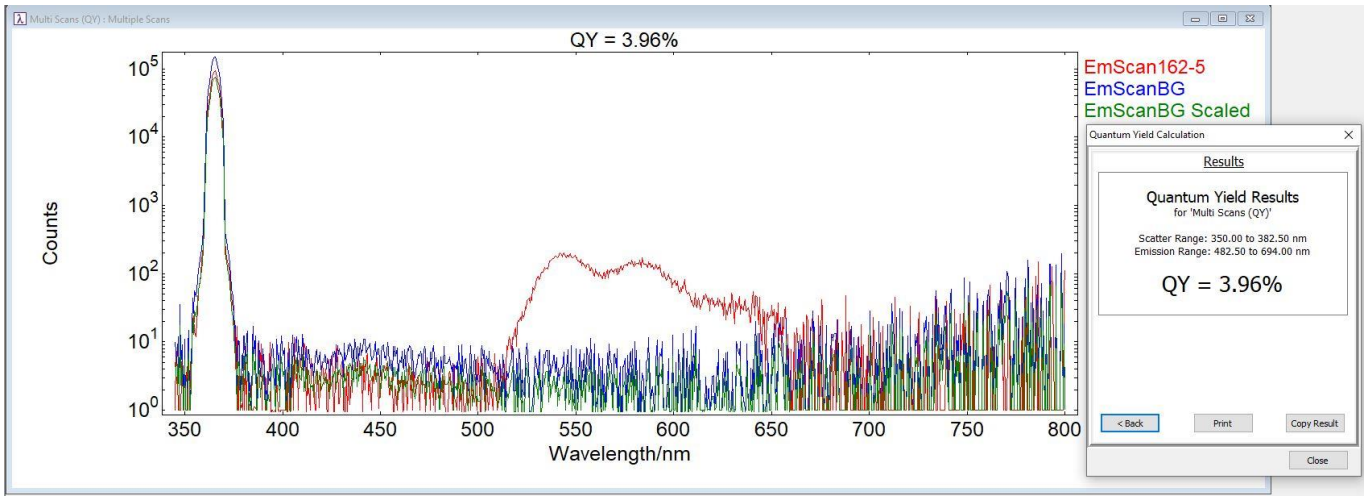

Figure S48. Absolute fluorescence quantum yield of complex **4a⊃P5** in CH_3CN.

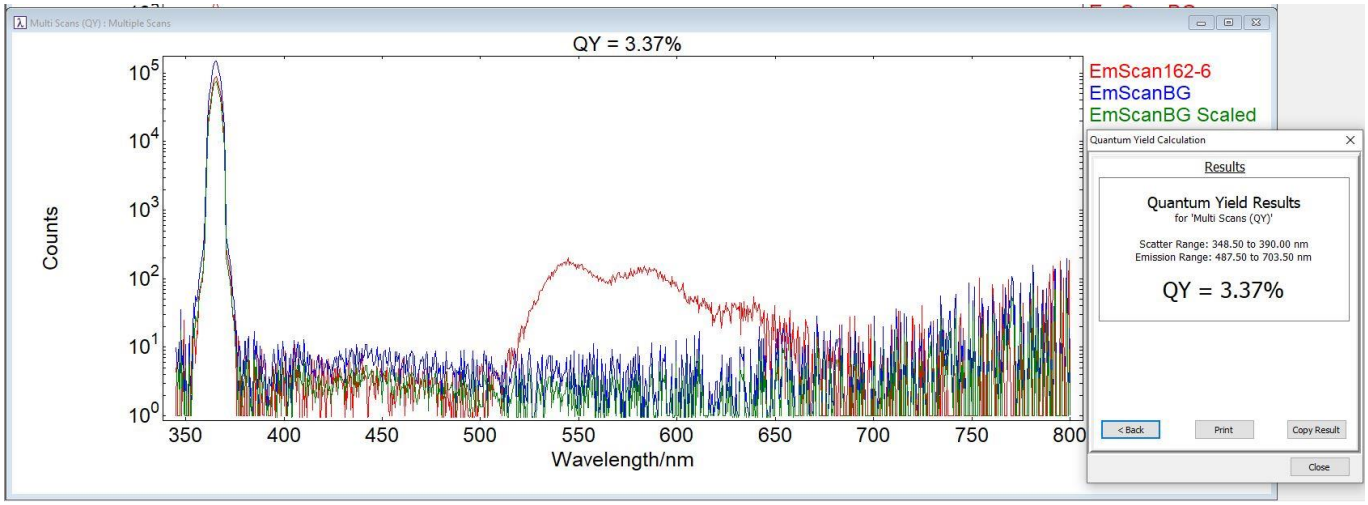

Figure S49. Absolute fluorescence quantum yield of complex **4a⊃P6** in CH_3CN.

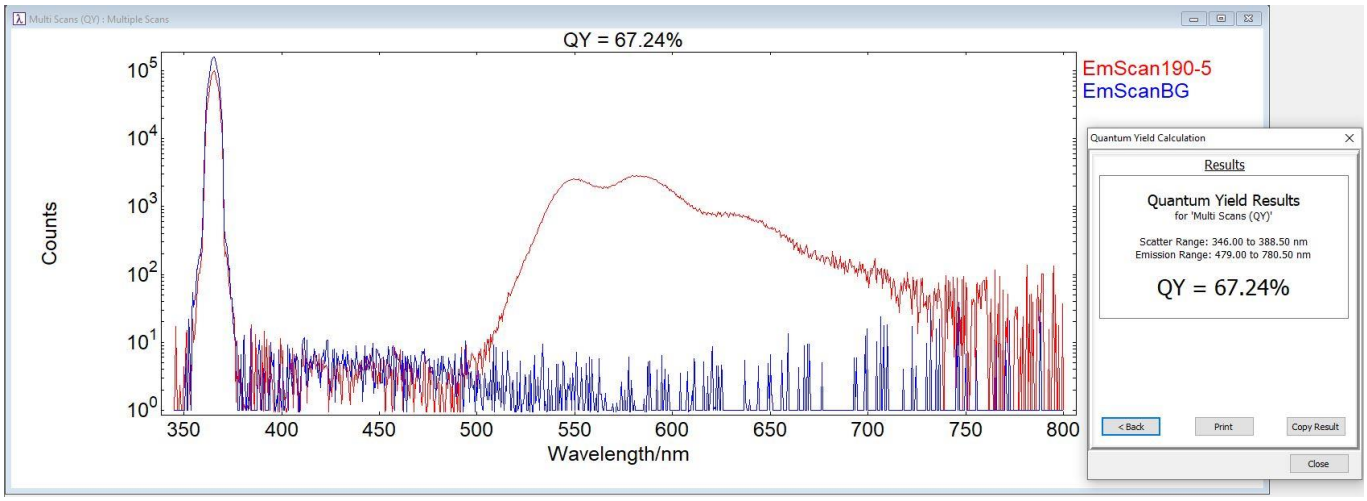

Figure S50. Absolute fluorescence quantum yield of complex **4b⊃P5** in CH_3CN.

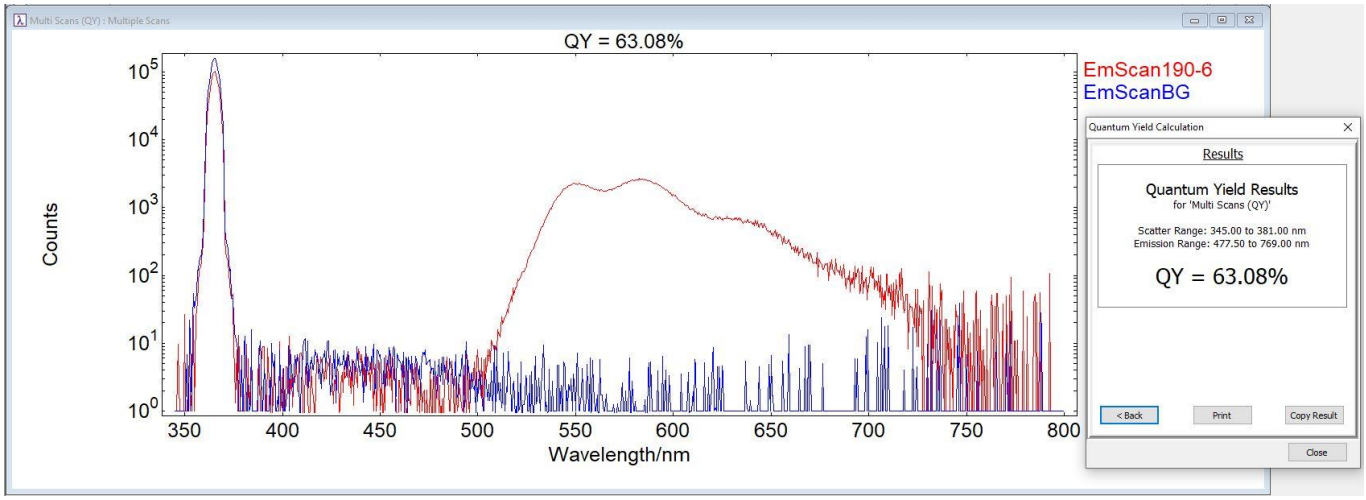

Figure S51. Absolute fluorescence quantum yield of complex **4b⊃P6** in CH_3CN.

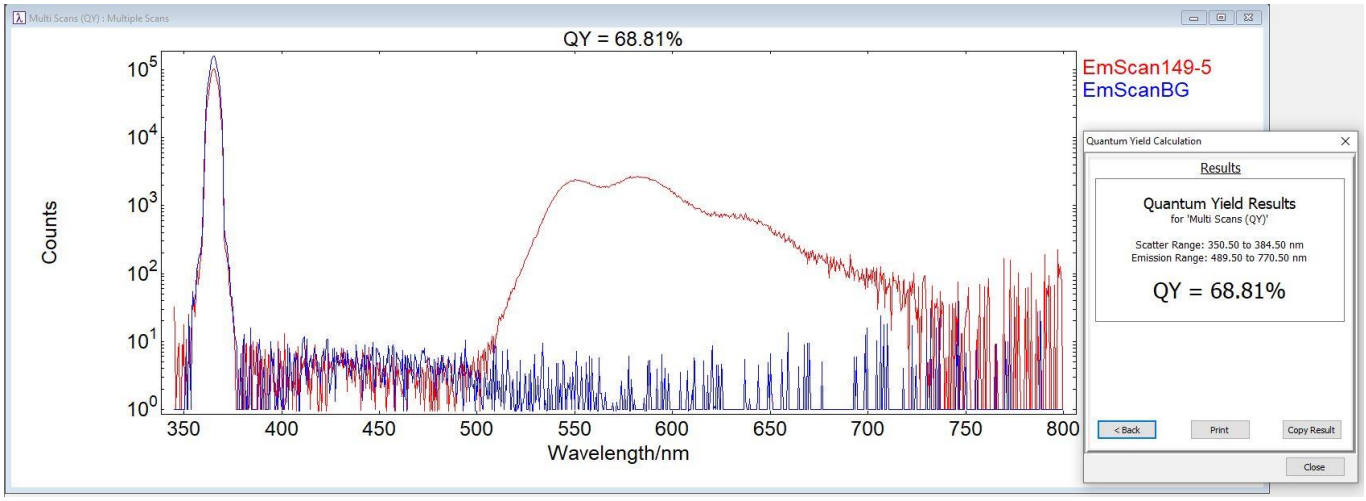

Figure S52. Absolute fluorescence quantum yield of complex **4c⊃P5** in CH_3CN.

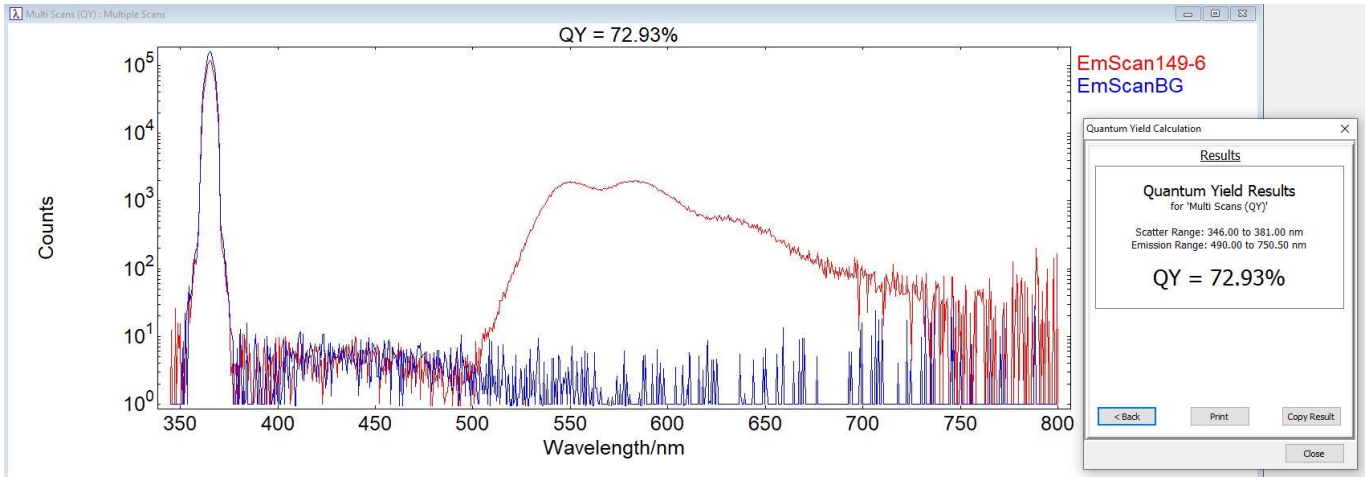

Figure S53. Absolute fluorescence quantum yield of complex **4c⊃P6** in CH_3CN.

7. *Study on the chiral transfer between host and guest*

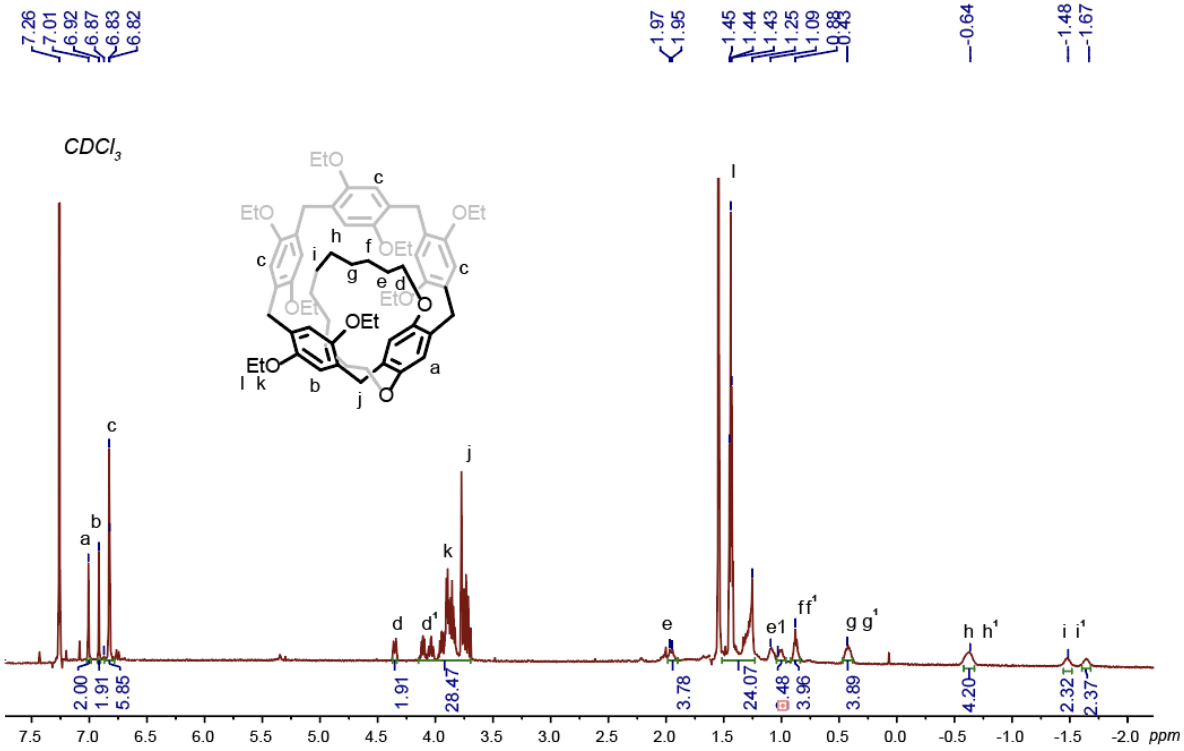

Figure S54. Partial ^{1}H NMR spectra (400 MHz, $CDCl_3$, 295 K) of pillar[5]arene-based molecular universal joint(**G1**).

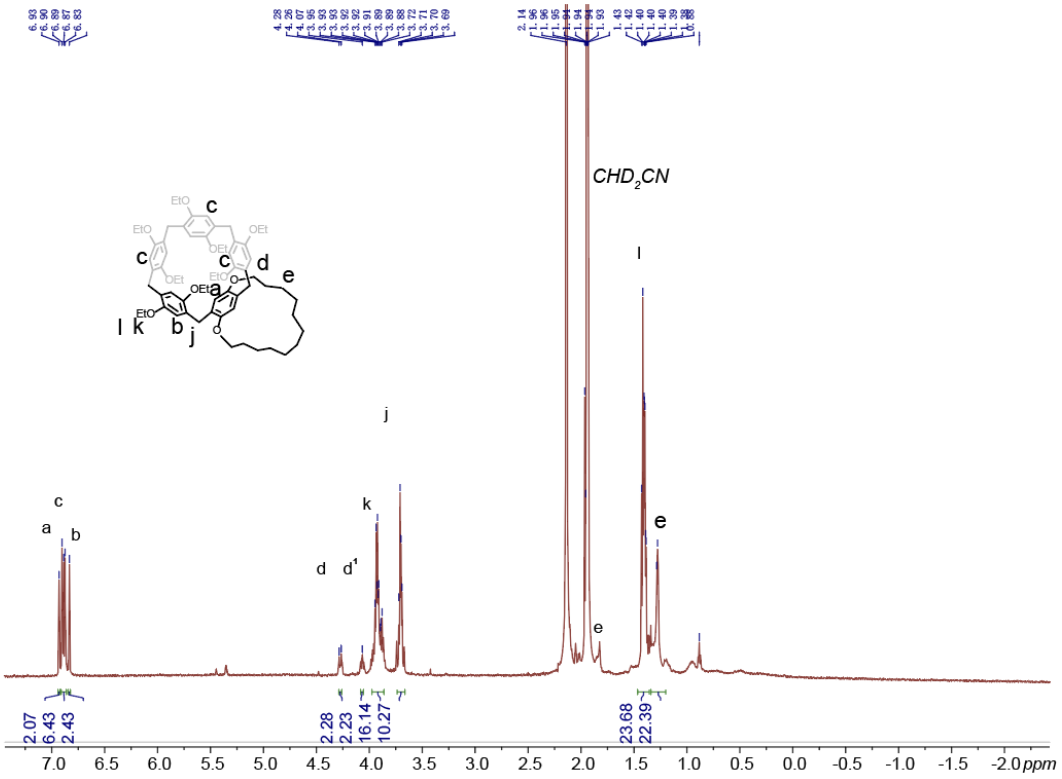

Figure S55. Partial ^{1}H NMR spectra (400 MHz, CD_3CN, 295 K) of pillar[5]arene-based molecular universal joint(**G1**).

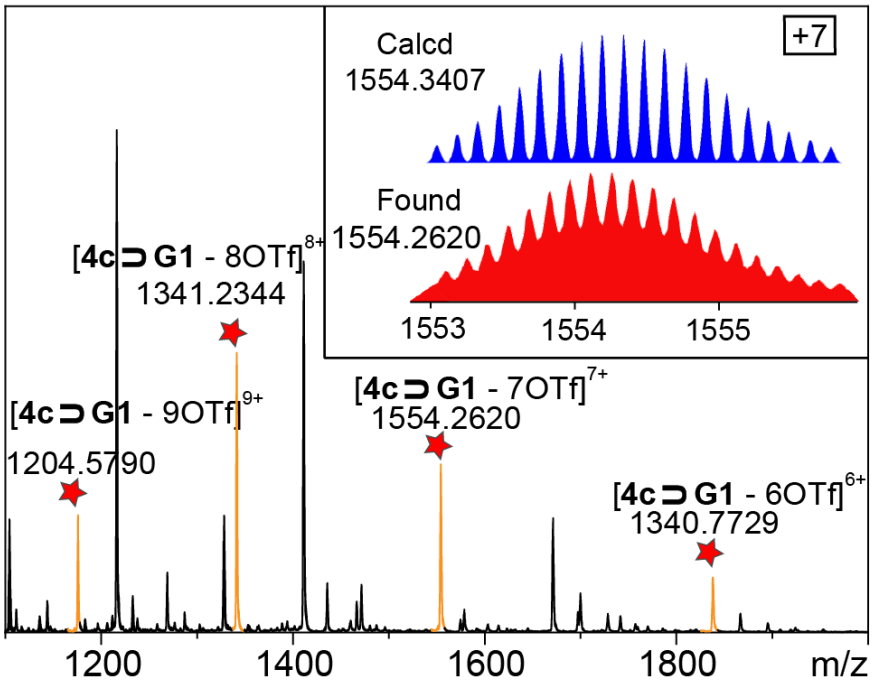

Figure S56. ESI-TOF-MS spectra of **4a**⊃G1.

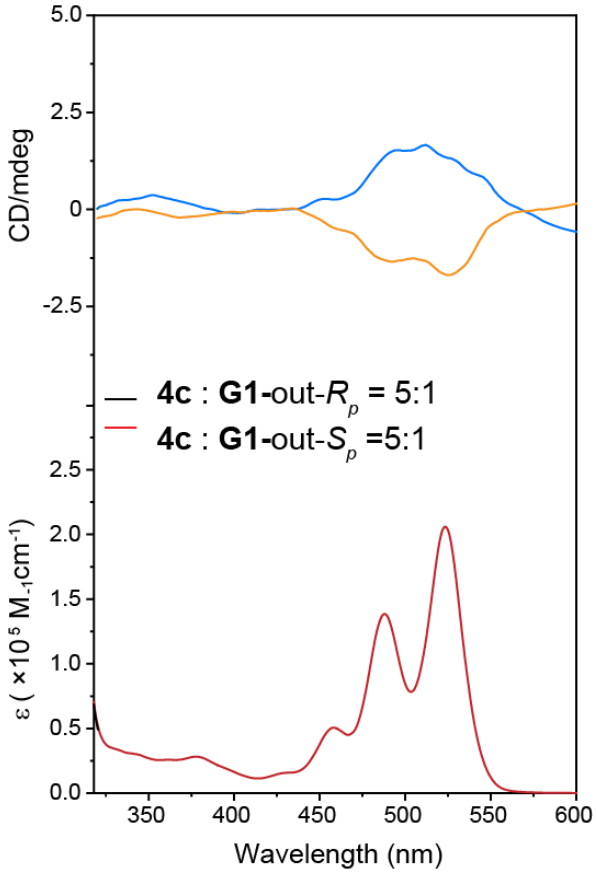

Figure S57. The CD of the host-guest complex **G1**- out-R_p and G1- out-S_p ($c_{\mathbf{G1}}$ = 2.5 × 10^{-6} mol L^{-1}) in CH_3CN at 298 K.

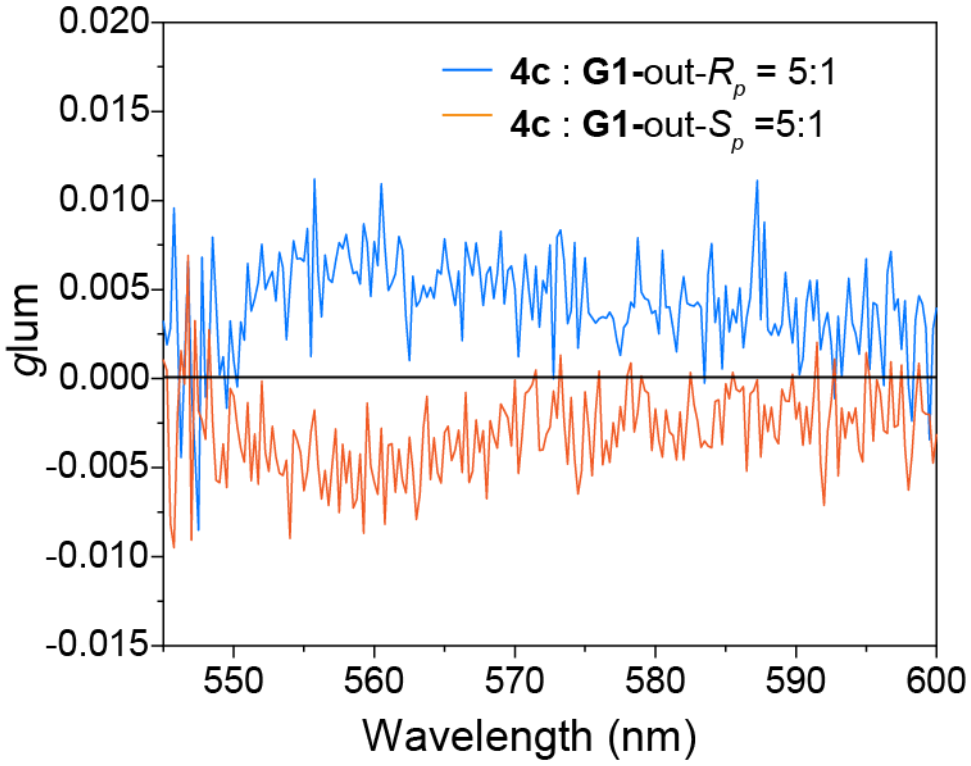

Figure S58. The *g*lum values of the host-guest complex **G1**-out-*R*p and **G1**-out-*S*p (c_{G1} = 2.5 × 10^{-6} mol L^{-1}) in CH_3CN at 298 K.

References

[S1] Y. Hou, Z. Zhang, S. Lu, J. Yuan, Q. Zhu, W.-P. Chen, S. Ling, X. Li, Y.-Z. Zheng, K. Zhu, M. Zhang, *J. Am. Chem. Soc*. **2020**, *142*, 18763..
[S2] http://app.supramolecular.org/bindfit/